HHS Public Access

Author manuscript

Biochim Biophys Acta Gene Regul Mech. Author manuscript; available in PMC 2024 September 01.

Published in final edited form as:

Biochim Biophys Acta Gene Regul Mech. 2023 September ; 1866(3): 194943. doi:10.1016/j.bbagrm.2023.194943.

Histone variant H2B.Z acetylation is necessary for maintenance of *Toxoplasma gondii* biological fitness

Laura Vanagas[1,*], **Daniela Muñoz**[1], **Constanza Cristaldi**[1], **Agustina Ganuza**[1], **Rosario Nájera**[1], **Mabel C. Bonardi**[1], **Valeria R. Turowski**[2], **Fanny Guzman**[3], **Bin Deng**[4], **Kami Kim**[5], **William J. Sullivan Jr.**[6], **Sergio O. Angel**[1,*]

[1]Laboratorio de Parasitología Molecular, INTECH, CONICET-UNSAM, Av. Intendente Marino Km. 8.2, C.C 164, (B7130IIWA), Chascomús, Prov. Buenos Aires, Argentina.

[2]Laboratorio de Bioquímica y Biología Celular de Parásitos, INTECH, CONICET-UNSAM, Av. Intendente Marino Km. 8.2, C.C 164, (B7130IIWA), Chascomús, Prov. Buenos Aires, Argentina.

[3]Núcleo de Biotecnología Curauma, Pontificia Universidad Católica de Valparaiso. Av. Universidad 330 Curauma, Valparaiso

[4]Department of Biology and VBRN, University of Vermont, Vermont, USA.

[5]Department of Internal Medicine, Morsani College of Medicine, University of South Florida, Tampa, FL 33612

[6]Department of Pharmacology and Toxicology, Indiana School of Medicine, Indianapolis, Indiana 46202, USA

Abstract

Through regulation of DNA packaging, histone proteins are fundamental to a wide array of biological processes. A variety of post-translational modifications (PTMs), including acetylation,

[*]Corresponding authors: Sergio O. Angel. Laboratorio de Parasitología Molecular, IIB-INTECH, CONICET-UNSAM, Av. Intendente Marino Km. 8.2, C.C 164, (B7130IIWA), Chascomús, Prov. Buenos Aires, Argentina. Tel.: +542241424303, sangel@intech.gov.ar (SO Angel) Laura Vanagas. Laboratorio de Parasitología Molecular, IIB-INTECH, CONICET-UNSAM, Av. Intendente Marino Km. 8.2, C.C 164, (B7130IIWA), Chascomús, Prov. Buenos Aires, Argentina. Tel.: +542241424303, vanagas@intech.gov.ar (L Vanagas).

Author Contributions: L.V. participated in all the experiments, analyses and design of the study and wrote the first draft; D.M. performed Crispr/Cas9 and some of the characterization experiments along with the pull-down experiments with L.V. supervision; C.C. performed the DNA damage experiments and some of the transfections; A.G. was involved in many of the experiments with technical support, and was in charge of RNA and cDNA preparation; R.N. performed RT-PCR experiments and ELISAs with LV supervision; M.C.B. performed Co-IP experiments with L.V. supervison; V.T. perfomed Rop5 and Rop18 antibodies and provided the respective primers for RT-PCR; F.G. synthesized biotynilated peptides for pull down experiments; B.D. performed mass spectrometry analysis; K.K. and W.J.S. participated in design of the study and manuscript final corrections; S.O.A. designed the study and participated in its supervision. All authors have read and agreed to the published version of the manuscript.

Institutional Review Board Statement: Not applicable.

Informed Consent Statement: Not applicable.

Declaration of Interests
All authors declare that there are no conflicts of interest.
There is no financial or non-financial assistance provided by a third party for the reported work.
There is no financial interest or relationship related to the subject matter.

Conflicts of interest: The authors declare that there are no conflict of interest.

constitute a proposed histone code that is interpreted by “reader” proteins to modulate chromatin structure. Canonical histones can be replaced with variant versions that add an additional layer of regulatory complexity. The protozoan parasite *Toxoplasma gondii* is unique among eukaryotes in possessing a novel variant of H2B designated H2B.Z. The combination of PTMs and the use of histone variants is important for gene regulation in *T. gondii*, offering new targets for drug development. In this work, *T. gondii* parasites were generated in which the 5 N-terminal acetylatable lysines in H2B.Z were mutated to either alanine (c-Myc-A) or arginine (c-Myc-R). The c-Myc-A mutant displayed no phenotype over than a mild defect in its ability to kill mice. The c-Myc-R mutant presented an impaired ability to grow and an increase in differentiation to latent bradyzoites. The c-Myc-R mutant was also more sensitive to DNA damage, displayed no virulence in mice, and provided protective immunity against future infection. While nucleosome composition was unaltered, key genes were abnormally expressed during *in vitro* bradyzoite differentiation. Our results show that regulation of the N-terminal positive charge patch of H2B.Z is important for these processes. We also show that acetylated N-terminal H2B.Z interacts with some unique proteins compared to its unacetylated counterpart; the acetylated peptide pulled down proteins associated with chromosome maintenance/segregation and cell cycle, suggesting a link between H2B.Z acetylation status and mitosis.

Keywords

Positive charge patch; cell cycle; differentiation; virulence; mitosis

Introduction

Histone proteins form nucleosomes that regulate packaging of DNA, thereby affecting DNA transcription, replication, and repair. In addition to the four canonical histones (H2A, H2B, H3 and H4), variant histones exist that can be substituted into the nucleosome, affecting its properties. Canonical and variant histones are also subject to a wide array of post-translational modifications (PTMs) that can alter the nucleosome or recruit chromatin remodeling machinery. The combination of PTMs and exchange of histone variants is believed to be important for gene regulation in the protozoan parasite *Toxoplasma gondii*, offering new targets for drug development [1–3].

T. gondii is a member of phylum Apicomplexa and infects between 10–90% of the population depending on the country [4], presumably influenced by dietary habits and environmental conditions [5]. *T. gondii* converts from rapidly growing tachyzoites, which cause acute infection, to slow or non-growing bradyzoites, which cause chronic infection and typically reside in the brain [6]. Although *T. gondii* infection is asymptomatic in healthy people, untreated clinical toxoplasmosis can be lethal in immunocompromised individuals such as transplant or HIV patients, and can produce severe disease during congenital infection, especially in early stages of development [7, 8]. Chronic toxoplasmosis has also been linked to brain tumor predisposition, attention-deficit/hyperactivity disorder, obsessive-compulsive disorder and schizophrenia [9–13].

The *T. gondii* life cycle is comprised of sexual and asexual stages. While sexual replication takes place only in felids, *T. gondii* is able to replicate asexually as tachyzoites in any nucleated cell in any warm-blooded vertebrate. Following infection, tachyzoites convert into bradyzoites, which are housed in tissue cysts that are impervious to immunity and current drug treatments. Recently, a myb-like transcription factor (BFD1) was described to be necessary and sufficient to induce bradyzoite differentiation [14]. How BFD1 is recruited to stage-specific promoters remains to be determined, but likely involves interplay with chromatin remodelers and epigenetic processes that include histone PTMs and/or variant histone exchange [15]. In support of this idea, treatment of tachyzoites with inhibitors of histone deacetylase 3 (HDAC3) initiates bradyzoite differentiation [16]. The roles of histone variants in *T. gondii* remain poorly understood.

We have previously shown that *T. gondii* expresses histone variants that mark functional regions of the genome [17]. H2A.Z is a ubiquitous variant that has been implicated in both transcriptional activation and gene silencing in eukaryotes; it also contributes to the regulation of DNA damage repair [18–20], which is an important process in *T. gondii* tachyzoites [21]. Unlike H2A.Z, most eukaryotes possess only specialized isoforms of H2B. By contrast, apicomplexan parasites [22–25] and trypanosomatids [26] contain H2B-like variants called H2B.Z and H2Bv, respectively, but their functions remain poorly understood.

Histones H2A.Z and H2B.Z form a dimer that localizes with the transcriptional activation mark H3K4me3 in promoter/transcriptional start site (TSS) regions surrounding the nucleosome-free region upstream of the transcription start site [17]. In addition, H2B.Z and H2A.Z localize to the gene bodies of silent genes, including repressed stage-specific genes, suggesting a role in the regulation of stage transitions. In *T. gondii*, both H2A.Z (TGGT1_300200) and H2B.Z (TGGT1_209910) are essential during the lytic cycle with CRISPR fitness scores of −5.08 and −4.05, respectively [27]. By mass spectrometry, both histone variants were found to be hyperacetylated at the N-terminal domain, whereas few or no acetylation marks were identified on canonical H2A, H2B and H2A.X [28]. *T. gondii* H2B.Z was shown to be acetylated at 5 lysine residues in its N-terminal tail. The H2A.Z N-terminal tail has 10 acetylatable lysines, in which lysine 18 can also be methylated [28]. H2A.Z N-terminal tail acetylation has been widely shown to be a hallmark for active chromatin whereas N-terminal methylation is associated with gene silencing [29–32], suggesting it is essential for changes in gene expression during cell differentiation [33–37]. While the role of N-terminal lysine acetylation in H2B.Z has not yet been studied, N-terminal acetylated canonical H2B is associated with some, but not all, active genes in vertebrates [38]. Interestingly, H2A.Z in most eukaryotes only bears 4–5 acetylatable lysine residues in the N-terminus, while in protists like *T. gondii, Plasmodium* or *Tetrahymena termophila*, this number is considerably higher (between 5 and 16). Moreover, *T. gondii* could harbor double variant nucleosomes that collectively contain 15 acetylatable lysines that could be involved in regulating chromatin and DNA proccesses.

In the present work we studied the role of the five *T. gondii* H2B.Z N-terminal lysines using a mutagenesis strategy; we also pursued a gene knockout strategy for H2B.Z. In an RH strain background, we generated *T. gondii* that possess mutated versions of H2B.Z: c-Myc-R, in which the five N-terminal acetylatable lysines were replaced by arginines, and

c-Myc-A, in which they were replaced by alanines. These lines were analyzed for their ability to grow *in vitro*, differentiate to bradyzoites *in vitro* and produce virulence in mice. In addition, expression of key genes was studied, as well as nucleosome composition and DNA damage sensitivity. Our results suggest that the aforementioned processes are regulated through the neutralization of the positive charge patch on the N-terminus of H2B.Z. We have also found some proteins that specifically interact with acetylated N-terminal H2B.Z peptide and not an unacetylated version, shedding new light on its role during the lytic cycle. The implications of these data on the putative role of H2B.Z is discussed.

Results

Sequence alignment of Apicomplexa H2B.Z N-tail

H2B.Z is a variant histone of the H2B family that appears early in the phylum Apicomplexa. Previously, it was observed that *T. gondii* and *Plasmodium falciparum* H2B.Z N-terminal tails contain five acetylated lysines (K4,K9,K13,K14, and K18) [28, 39, 40]. The conservation of the five acetylatable lysines is clear from the alignment of H2B.Z N-terminal tail sequences from different Apicomplexa (Fig. 1A). This profuse number of modifications in the N-terminal tail, concomitant with the nucleosome partner, H2A.Z, in which several acetylatable lysines are present, make this double variant nucleosome a likely feature for chromatin modification relevant to gene expression, replication, and/or DNA damage responses.

Overexpression of tagged wild type and mutant versions of H2B.Z and knockout of endogenous *H2B.Z*

Attempts to knockout *h2b.z* through genetic deletion were unsuccessful (data not shown). The failure to obtain an H2B.Z. knockout is consistent with its CRISPR fitness score of −4.05, strongly suggesting it is essential for parasite viability [27] (ToxoDB, TGGT1_209910).

Given the high number of modifiable lysines in the H2B.Z variant unique to apicomplexan parasites, we analyzed their role by ectopically expressing myc-tagged wild-type or mutant forms. We generated parasites over-expressing wild-type H2B.Z (c-Myc-WT-OE) or a mutated form in which all the acetylatable lysines in the N-terminal tail were changed to alanine, which mimics how acetylation ablates the positive charge of the lysine residues. We also over-expressed a mutated version in which the lysines were replaced with arginines, generating a positive charge patch that could no longer be neutralized by acetylation (Fig. 1B). Neither of these mutants can be acetylated in this region, rendering them incapable of interacting with bromodomain proteins, mediators of the histone code. Correct localization of each c-Myc-H2B.Z protein was checked by immunofluorescence assay (IFA) (Fig. S1A) and by western blotting, which revealed the expected two bands in the over-expressing lines (Fig. S1B). To note, c-Myc-WT-OE was already used in a ChIP seq screen, showing the same genomic localization as endogenous H2B.Z when the experiments were performed using α-H2B.Z antibody [17].

We then deleted the endogenous *H2B.Z* gene using CRISPR methodology in lines overexpressing c-Myc-H2B.Z mutants (Fig 2A). We took advantage of the number of mutations in the N-terminal tail of the tagged version to design sgRNA specific for endogenous *H2B.Z* gene. Using this strategy, we obtained *T. gondii* RH lines expressing only c-Myc-tagged H2B.Z with its corresponding N-terminal mutations, denoted c-Myc-A and c-Myc-R (Fig. 2A–C, Fig. S1C–D). Each form of c-Myc H2B.Z in these parasites localized properly to the nucleus (Fig. 2B) and displayed a single band corresponding to the mutant c-Myc-H2B.Z probed by western blot with anti-H2B.Z or anti-c-Myc antibodies (Fig. 2C). Quantification of the c-Myc-H2B.Z band relativized to Sag1 as a control showed comparable levels of expression between mutants (1.43 ± 0.77 and 1.65 ± 0.82 for c-Myc-R and c-Myc-A, respectively).

In vitro growth analysis in c-Myc-R and c-Myc-A *T. gondii* lines

We used a competitive growth assay to determine differences in parasite growth between parental wild-type and mutant parasites (c-Myc-A and c-Myc-R). Approximately equal amounts of c-Myc positive and c-Myc negative (parental) tachyzoites were mixed and allowed to invade hTert host cells, which were then analyzed by IFA on different days post-infection. While the c-Myc-A parasites showed no change in growth relative to the parental line over time, the c-Myc-R line showed a marked growth deficiency compared to the parental line (Fig. 3A). As arginines conserve the positive charge and cannot be acetylated, these results indicate that the constitutive positive charge patch on the H2B.Z N-terminal tail impairs tachyzoite growth *in vitro*. Therefore, wild-type *T. gondii* must regulate the charge patch on H2B.Z N-terminal tail by PTMs such as acetylation for normal growth.

In vitro differentiation analysis in c-Myc-R and c-Myc-A *T. gondii* lines

We next studied the effect of the mutant H2B.Z variants on *in vitro* tachyzoite to bradyzoite differentiation using alkaline stress to trigger stage conversion and *Dolichos biflorus* lectin (DBL) to monitor tissue cyst wall formation. Strikingly, we found that c-Myc-R, but not c-Myc-A, showed an increase in DBL-positive vacuoles compared to the wild-type control (Fig. 3B), suggesting that the positive charge patch on the H2B.Z N-terminal tail may be involved in bradyzoite differentiation. The inability to neutralize the H2B.Z charge patch (e.g. through acetylation) may facilitate cyst formation.

We also checked whether key stage-specific genes were altered in parasites expressing mutant H2B.Z. We obtained RNA from freshly lysed tachyzoites, early bradyzoites (48 hours post-differentiation), and late bradyzoites (96 hours post-differentiation) of the parental RH strain and c-Myc-A or c-Myc-R parasites. We analyzed the expression of *Sag1* (tachyzoite), *Bag1* (early bradyzoite), *LDH2* (early bradyzoite), *AP2IX-9* (mature bradyzoites) [41], *AP2 IV-3* (in which expression is maximal at 48h post-differentiation, decreasing in mature bradyzoites) [42], and *BFD1* [14] mRNA by RT-qPCR. Actin and tubulin were used as housekeeping genes, and data were normalized to actin. The amount of expression relative to tachyzoite in each parasite line is plotted, showing a trend of expression in c-Myc-R similar to what would be expected for a cystogenic (type II) strain, and different from an RH (type I) expression profile (Fig. 3C). Also, *BFD1* mRNA was

increased in the c-Myc-R mutant, compared to wild-type RH (Fig. 3C). Notably, the expression profile of BFD1 in RH type I strain has not been published to date. These results are consistent with the heightened bradyzoite differentiation rate seen in c-Myc-R parasites.

Sensitivity to DNA damaging agents in c-Myc-A and c-Myc-R lines

In other species, H2A.Z has been linked to DNA double-strand break repair driven by the non-homologous end joining (NHEJ) pathway [20, 43, 44]. Consequently, H2A.Z contributes to the response against the genotoxic effects of hydroxyurea (HU) or methyl methanesulfonate (MMS) [44]. We have previously characterized the antiparasitic activities of MMS, HU, and campothecin (CPT) in *T.gondii* [45]. Topotecan is a genotoxic drug, an analog to CPT that produces fork collapse and ulterior DNA double-strand breaks repaired by homologous recombination repair (HRR) [46].

Given the roles of histone variants in DNA repair, we analyzed c-Myc-A and c-Myc-R parasites for sensitivity to topotecan at its IC_{50} value (20 μM, unpublished results) and MMS (50 μM) using the competitive growth assay. We observed a significative decrease in growth compared to the parental only after treatment with MMS in c-Myc-R tachyzoites (Fig. 4A). By contrast, topotecan did not produce a significant defect in growth, although c-Myc-R seems to be more sensitive (Fig. 4A). In addition, treatment with MMS produced disorganized vacuoles, rounded parasite shapes, and a loss of genetic material in both mutants as well as parental lines (Fig. 4B). Treatment with MMS and Topotecan also produced asynchronous replication, leading to unusual number of tachyzoites within parasitophorous vacuoles (PV) (Fig. 4B). For both DNA-damaging agents, these anomalous PVs were significantly more abundant in c-Myc-R compared to parental and c-Myc-A (Fig. 4C). Taken together, the constitutive positive charge patch on H2B.Z in the c-Myc-R parasites alters the DNA damage response to MMS, suggesting that acetylation status of H2B.Z N-terminal tail is likely to be modulated for proper DNA repair.

In vivo analysis in c-Myc-R and c-Myc-A *T. gondii* lines

Proper gene regulation is required for tachyzoite propagation in different tissue environments and differentiation *in vivo*. Progression of tachyzoite infection of these mutants was analyzed in C57BL/6 mice by inoculating 100 tachyzoites per *T. gondii* line. As expected, parental parasites displayed high virulence, killing mice within 7 days (Fig. 5A). c-Myc-A tachyzoites were also lethal to mice, but with a delay in the time of death (Fig. 5A). According to Mantel-Cox and Gehan-Breslow-Wilcoxon tests, the survival curves are significantly different ($p>0.0001$), suggesting that acetylation of at least some of the 5 N-terminal tail lysines is relevant for parasite progression *in vivo*.

In contrast, c-Myc-R and Me49 infected mice, as well as non-infected (PBS group) survived until sacrifice on day 30–35 (Fig. 5A). c-Myc-WT-OE was used a control to show that the tagged version of H2B.Z is not responsible of affects observed. *T. gondii* lines expressing both endogenous H2B.Z and c-Myc-H2B.Z-R (c-Myc-R-OE), were as lethal as the parental line (data not shown), suggesting that the randomly integrated ptub-*H2B.Z-R* gene is not responsible for the loss of virulence and that co-expression of wild-type H2B.Z and the H2B.Z-R mutant histone did not generate a dominant negative effect. Infection with 1,000

and 10,000 c-Myc-R tachyzoites were also nonlethal to mice, underscoring its profound fitness defect *in vivo* (Fig S2A).

To confirm acute infection took place, hematoxylin and IFA staining of the peritoneal fluids at day 4 post-infection was performed (Fig. 5B). Intraperitoneal tachyzoites could be detected with parental and c-Myc-A *T. gondii* lines but not with c-Myc-R parasites (Fig. 5B). Surviving animals (those infected with c-Myc-R and Me49 *T. gondii* lines) were screened for antibodies against *T. gondii*. An increase in total IgG in mice infected with c-Myc-R tachyzoites was observed, comparable to Me49, which indicated that an initial infection had taken place (Fig. 5C, Fig. S2B). The analysis of IgG subtypes showed a Th1-like humoral response in both cases, associated to IgG2a and higher for IgG2b (normal for C57/BL6 mice), typical for an intracellular parasite infection (Fig. 5C, Fig. S2B). Following sacrifice, brains of surviving mice were processed for cyst detection by direct observation with optical microscopy and DBL staining. Tissue cysts were observed in brains of mice infected with Me49 strain, but not in those infected with c-Myc-R parasites (data not shown).

To determine if c-Myc-R parasites elicit an adequate immune response to protect against a subsequent challenge infection, mice previously infected with 1,000 c-Myc-R tachyzoites were re-infected with 100 tachyzoites of the highly virulent RH parental line 30 days later. c-Myc-R infected mice survived until sacrifice, while all mice in the control group died at day 38 (day 8 after re-infection) (Fig. 5D). These results suggest that c-Myc-R tachyzoites stimulate a robust cellular immune response that is sufficient to control a challenge infection.

H2B.Z acetylation status is involved in regulation of ROP protein expression

The ability of the c-Myc-R line to establish a protective immune response suggests that these parasites can invade host cells but are efficiently controlled by the immune system. Among the *T. gondii* virulence proteins that exert protection from PV establishment are the polymorphic rhoptry proteins Rop5 and Rop18, which disrupt the γIFN-inducible IGR pathway [47–51]. Here, we used antibodies against *T. gondii* Rop5 (TGGT1_411430) and Rop18 (TGGT1_205250) recombinant proteins for western blot analysis. Rop5 was present in parental, c-Myc-A, and c-Myc-R parasites, whereas Rop18 was only detected in the parental line (Fig. 6A). However, quantification of the band intensities showed a significant decrease in Rop5 abundance in c-Myc-R parasites and a lack of Rop18 protein in both c-Myc-A and c-Myc-R (Fig. 6B and Fig. S3A). To test whether the absence of Rop18 was a consequence of the insertion of the H2B.Z construction in that locus, we performed the same experiment using the over-expressing tachyzoites obtained prior to CRISPR mediated knockout of endogenous H2B.Z. As shown in Fig.S3B, C, both Rop5 and Rop18 are detectable in every clone similar to parental. Co-localization analysis showed a correct localization of Rop5 in all *T. gondii* lines whereas Rop18 could only be detected in the parental line (Fig. 6C). Of note, we also detected a decrease in the fluorescence intensity of Rop5 in c-Myc-R parasites (Fig. 6D). RT-PCR analysis indicated that both genes were expressed in every *T. gondii* line (Fig. S3D), suggesting that alteration of Rop5 and Rop18 expression in the c-Myc-R line is likely at the post-transcriptional level.

Double variant nucleosome and transcription is not altered in *T. gondii* mutant lines in normal conditions

Since H2B.Z is part of a double variant nucleosome with H2A.Z, which localizes at the promoter region of active genes, it was expected that expression alterations would occur at the transcriptional level rather than post-trancriptionally. To determine if the observations for Rop5 and Rop18 were a specific situation, we looked closer at the role of H2B.Z in transcription. We first analyzed the double variant (H2A.Z/H2B.Z) formation in both mutant lines by co-immunoprecipitation (co-IP) assays with H2B.Z antibody or commercial anti-c-Myc agarose. Mononucleosomes of c-Myc-A and c-Myc-R lines were obtained after MNAse digestion before co-IP (Fig. S4A). Figure 7A shows that both c-Myc-A and c-Myc-R H2B.Z mutants interact with H2A.Z, confirming the assembly of the double variant nucleosome already found in *T. gondii*. It is also shown that the IP worked correctly by c-Myc immunoreactivity in the WB (Fig. 7A). We also decided to study the interaction of the double variant nucleosome with acetylated H3, a known mark of active chromatin. Both c-Myc-A and c-Myc-R H2B.Z interacted with this acetylated histone, which indicates that lack of acetylation of H2B.Z does not alter this PTM crosstalk (Fig. 7A and Fig. S4C, D). Co-IP performed by using pre-immune serum as a control shows no reactivity with any of the antibodies assayed (Fig. S4B). Quantification of the IP band intensities relative to the respective input band showed that both *T. gondii* lines exhibit similar interaction levels with H2A.Z and acetylated H3 (Fig. 7B). These data indicate that the mutant H2B.Z histones did not alter the ability to form double variant nucleosomes with H2A.Z, nor their interaction with the open chromatin marker, acetylated H3.

We next decided to explore if transcription was altered in tachyzoites of the mutant lines. We analyzed expression of *Sag1* (tachyzoite), *tubulin* (constitutive), *Bag1* and *LDH2* (bradyzoite) and *BFD1* (master differentiation factor). Only BFD1 mRNA expression was statistically higher in c-Myc-R that in the parental or c-Myc-A (Fig. 7C), consistent with our observation that c-Myc-R parasites are more prone to differentiate into bradyzoites.

Chromatin compaction does not explain differences observed in *T. gondii* mutant lines

The positive charge patch on H2B.Z could be associated with a more compact chromatin structure. To analyze chromatin compaction, we measured the size of the nuclei in H2B.Z mutant parasites compared to the parental in IFAs co-stained with DAPI and α-H2B.Z antibody. As shown in figure 7D, nuclei sizes are significantly smaller than the parental in c-Myc-R parasites in accordance with the hypothesis. However, this significant difference is also seen in c-Myc-A tachyzoites, indicating that the inability of this histone to be post-translationally modified is enough to lead to this state. Note that nuclei size in c-Myc-WT-OE parasites are similar to parental nuclei, indicating that c-Myc tag is not responsible for this effect (Fig. 7D). These findings suggest that acetylation of the H2B.Z N-terminal tail could be required for proper control of DNA compaction status, but we cannot dismiss that mutating lysines to alanines or arginines may have induced structural effects that altered the compaction state of chromatin.

H2B.Z interacting proteins

While results largely implicate the positive charge patch of H2B.Z N-terminal tail as responsible for the observed phenotypes, a role for acetylation cannot be ruled out. In fact, the lack of acetylation in the N-terminal lysines could be one of the causes why the c-Myc A line showed a mild defect in virulence *in vivo* and defects in chromatin compaction. These defects could be associated by disrupting the interactions of H2B.Z with acetylation "readers" (e.g. bromodomain proteins). We therefore examined if there are differential proteins interacting with H2B.Z N-terminal region depending on its acetylation state. We designed two peptides, one containing two acetylated lysines (K14 and K18) and the other unacetylated; both peptides contained a biotin tag towards the C-terminal end. Peptide design was performed according to Wysocka 2006 [52]. According to this work, we performed the synthesis of peptides about 20 amino acids long, with biotin conjugated through a linker on the C-terminus, and with the modification positioned close to the center of the peptide. In addition, two consecutive modifications were not recommended, explaining our choice of K14 and K18.

We used extracellular tachyzoites (RH) to perform the pull-down assays. After resolving on SDS-PAGE, samples were analyzed by mass spectrometry. We detected a total of 48 interactors, 18 exclusive to the non-acetylated oligo, 17 exclusive to the acetylated oligo, and 14 present in both (Table S1). While many interactors are nuclear proteins, others were non-nuclear, with many being typical contaminants (e.g. ribosomal subunits). Among the nuclear proteins, several may be interacting with the H2B.Z N-terminal tail independent of acetylation status, such as GCN5-A, histone H4, and a PHD protein (Table 1). Three nuclear proteins were differentially pulled down repeatedly across two independent experiments: RRM protein TGME49_262620 (pulled down with the unacetylated peptide), H3.3, and a putative CDK protein (both pulled down with the acetylated peptide). Considering the nuclear genes that only appeared in one pull down, the acetylated peptide retrieved only proteins associated with the maintenance and segregation of chromosomes during the cell cycle, including peptidase c50 (TGME49_262825), RecF/RecN/SMC N terminal domain-containing protein (TGME49_231170) and meiotic recombination protein DMC1 family (TGME49_216400) (Table S1). Among the retrieved peptides in both acetylated and non-acetylated pull-downs, we also detected an apicoplast localized acetyl-CoA carboxylase ACC1 (TGME49_221320) (Table 1 and Table S1). It requires further examination, but such an interaction suggests that H2B.Z may be present outside the nucleus, which has been observed in other eukaryotes [53–57].

Discussion

In *T. gondii*, the proper regulation of gene expression is crucial for progression through the cell cycle, lytic cycle, and stage differentiation [15, 58–63]. Chromatin remodeling is a major contributing factor in the regulation of gene expression and is mediated in part by histone variant exchange and histone PTMs. In addition to regulating chromatin, these processes affect chromosomal organization, DNA repair, and DNA replication [64]. Apicomplexan parasites possess a unique double variant nucleosome configuration composed of H2A.Z/H2B.Z, which is extensively modified by PTMs including N-terminal

tail acetylation. The *T. gondii* epigenome has shown that this parasite uses a set of different histone modifications as a complex set of tools to control its gene expression [65]. Acetylation and methylation mediate opposing effects on gene expression, the first favoring expression and the second often favoring repression. As an example, acetylation of lysine 31 on histone H4 (H4K31) has been associated to the promoters of active genes, while in the core body of these genes H4K31me1 is found [64]. *T. gondii* H2B.Z/H2A.Z double variant nucleosomes are found in the promoter of active genes and in the gene body of inactive genes [17]. This disparity in genomic location could be regulated by the different PTMs of H2B.Z and/or H2A.Z. The present work is the first attempt to decipher the role of the N-terminal acetylation of H2B.Z.

Using an H2B.Z K-R mutant, our data show that constitutive positive charge patch in the N-terminal tail causes a decrease in growth, an increase in differentiation, and an impaired DNA damage response *in vitro*. In addition, *in vivo* virulence in mice was severely attenuated, an effect that was much milder in a H2B.Z alanine mutant. Similar studies were performed in *T. termophila*, in which constitutive positive charge patch engineered on H2A.Z proved highly toxic, suggesting that its regulation has an essential function [66]. Moreover, the presence of a single acetylation site in this region was sufficient to avoid the toxic effect of the positive charge patch [66, 67]. In *T. gondii*, which remain viable *in vitro*, when H2B.Z lysines are replaced by arginines, it is possible that effects of the constitutive positive charge patch of H2B.Z are partly mitigated by H2A.Z, which contains 10 acetylatable lysines [28]. Together, H2A.Z/H2B.Z possesses of 15 potentially modifiable lysines in their N-terminal tails. Future study of acetylation on the H2A.Z N-terminal tail is needed to better characterize the function of this double variant nucleosome.

The *T. gondii* c-Myc-R was more sensitive to MMS-mediated DNA damage *in vitro*, suggesting that the positive charge patch of H2B.Z plays a role. Since H2B.Z is unique to Apicomplexa, we can only infer the putative role of this variant histone in the context of the H2A.Z/H2B.Z nucleosome. The participation of H2A.Z in DNA damage repair pathways has been studied in mammals and yeast [20, 43, 44]. In those cases, H2A.Z was found to be involved in repair following exposure to genotoxic agents such as MMS and HU [44]. In our case, H2B.Z only demonstrated sensitivity with MMS and not with topotecan, supporting the possibility that H2B.Z/H2A.Z work together in the same function.

While c-Myc-R parasites showed a fitness defect *in vitro*, they had an even stronger defect *in vivo*, failing to produce a robust infection in mice. This H2B.Z mutant line appears capable of host cell invasion, sufficient enough to generate an immune response, but it is quickly controlled by the animal. The greater defect in mice is likely due to the harsher environment encountered *in vivo*, compared to *in vitro*. These pressures would include adaptation to new environments, including different cell types and organs, which may present differences in metabolism, nutrient availability, or immune responses. Under these conditions, where the tachyzoite must respond quickly, fine reprograming of gene expression and modifications in metabolic pathways would be required and the impossibility of modulating the positive charge patch of H2B.Z could hamper the ability of parasites to adapt to rapidly changing environments *in vivo*.

We considered that the changes provoked by making the H2B.Z N-tail constitutively positive charged could be related to alterations in chromatin compaction. Expansion of genome size during eukaryotic evolution has led to an increase in arginines in the H2A N-terminal tail. Arginine-rich histones bind more tightly to DNA, compacting chromatin and, in some cases, the nuclei are smaller as result [68]. However, in this work we showed that nuclei size was smaller in both c-Myc-R and c-Myc-A parasites compared to parental and to c-Myc-WT-OE tachyzoites, indicating that charge in the N-terminal tail is not responsible for chromatin compaction. Considering that changes in the primary sequence of histones could affect their function independently of modifications like acetylation, conducting structural analyses of both mutants could help clarify these results. Chromatin compaction has also been described to be regulated by linker histone H1, which stabilizes nucleosome structures. A candidate H1 has been recently identified in *T. gondii*, and interaction of H1 with H2B.Z was observed [69]. The acetylation status of H2B.Z may be important for this interaction, leading to more compacted chromatin in both alanine and arginine mutants because of linker histone H1. Further experiments are needed to test this hypothesis.

We also considered that the phenotypic alterations observed were due to defects in nucleosome formation, with a subsequent impact on gene expression. Our findings did not support this idea, although a full transcriptomic analysis would be more informative. We did show that changes in Rop5 and Rop18 do not occur at the transcriptional level, but rather post-transcriptionally. This regulation could be mediated by the presence of non-coding RNAs (ncRNAs) and there is increasing evidence for a significant role for postranscriptional mechanisms [70, 71]. Future studies should take this possibility into account, considering a possible role of H2B.Z acetylation, to analyze ncRNAs expression in *T. gondii*. With the results shown in this work it is only possible to correlate the decrease in one of the more virulent isoforms of Rop5 together with the absence of Rop18 protein to the loss of virulence of c-Myc-R mutant, although it cannot be ruled out that other virulence factors could be altered in these parasites. On the other hand, the absence of Rop18 protein in c-Myc-A correlates with the significant delay in mouse death with c-Myc-A infection as reported by Reese et al [49].

We could not detect significant changes in most of the genes analyzed by RT-qPCR under normal tachyzoite conditions, with exception of *BFD1* in c-Myc-R parasites. This does not rule out an association of the N-terminal tail of H2B.Z with epigenetic modulation of gene expression in some circumstances; for example, the changing environments, such as those encountered *in vivo*. Regarding the significant expression of BFD1 mRNA, it is likely to underlie the high differentiation rate observed for c-Myc-R parasites. It is important to note that BFD1 mRNA has been found constant across different stages and stress triggers translation [14]. Therefore, the increase in transcription *per se* is not enough to induce differentiation, but the higher levels of BFD1 mRNA could favor differentiation under alkaline stress. There is also another possibility of inducing differentiation based on epigenetic regulation. HDACi FR235222 treatment was shown to favor acetylation of H4K31ac in bradyzoite gene promoters, promoting transcription of bradyzoite genes and therefore, bradyzoite development [64]. Maybe under differentiation stress, H2B.Z functions to fine tune gene expression through the acetylation level of its N-terminal tail. Keeping that

in mind, the lack of modulation of H2B.Z in c-Myc-R could result in a different chromatin configuration that activates expression of bradyzoite-specific genes under alkaline stress.

Acetylated and unacetylated H2B.Z peptides both pulled-down three nuclear proteins: GCN5-A, a PHD finger protein, and clathrin. In other species, GCN5 affects H2A.Z acetylation via crosstalk with H4 acetylation by means of the bromodomain in p300 [72]. The unacetylated peptide recognized one protein specifically, an RNA recognition motif (RRM)-containing protein (TGME49_262620), which was also pulled down with GCN5b acetyltransferase in another study [60]. RRM-containing proteins are involved in post-transcriptional gene expression processes, such as mRNA and rRNA processing, RNA export, translation, localization, stability, and turnover [73]. The acetylated peptide pulled down two specific proteins: a cyclin-dependent kinase regulator (CDK; TGME49_219832) and H3.3 histone variant (TGME49_218260). CDKs phosphorylate multiple substrates that regulate the cell-division cycle in response to different cellular cues [74]. H3.3 and H2A.Z are associated with promoter regions flanking the nucleosome depleted region (NDR) of active genes [75]. Therefore, it may be likely that acetylated H2A.Z and H2B.Z would associate with this variant histone in active promoters. However, this association was not found in our genome-wide analysis of the tachyzoite stage [17].

In addition, CDKs have also been linked to mitosis [76, 77] and H3.3 is related to chromosome segregation, nuclear structure, and the maintenance of genome integrity [78]. Notably, our pull-down assay has also retrieved, only for the acetylated peptide, other genes associated with chromosome segregation (Table S1). Among them, peptidase c50 (TGME49_262825) a separase or caspase-like protease, known to play a central role in the chromosome segregation [79]. Structural maintenance of chromosomes (SMC) proteins -like RecF/RecN/SMC N terminal domain-containing protein (TGME49_231170)- function together with other proteins in a range of chromosomal transactions, including chromosome condensation, sister-chromatid cohesion, recombination, DNA repair and epigenetic silencing of gene expression [80–82]. Finally, meiotic recombination protein DMC1 family (TGME49_216400) proteins participate in meiotic recombination, specifically in homologous strand assimilation, which is required for the resolution of meiotic double-strand breaks [83]. These findings open an interesting question that could implicate a role of H2A.Z/H2B.Z in the process of mitosis and chromosome segregation.

It is relevant that c-Myc-R tachyzoites were able to generate a complete immune response, which only happens when cells are invaded by tachyzoites, not following infection with dead or lysed tachyzoites [84–87]. Toxovac® is a live attenuated vaccine used in sheep to prevent congenital toxoplasmosis [88]. Recently, a Ca^{2+}-dependent protein kinase (CDPK) knock-out in Me49 type II strain was evaluated in mice as a potential vaccine candidate [89]. Inoculation in mice with c-Myc-R parasites did not produce significant illness, protected from a subsequent challenge infection, and left behind no detectable brain cysts. This result suggests c-Myc-R parasites could be a useful vaccine candidate against toxoplasmosis.

In conclusion, our findings highlight the crucial role of H2B.Z in regulating biological processes such as growth, differentiation, and infection in *T. gondii* through the acetylation of positive charges in its N-terminal tail lysines. This underscores the significance of

H2B.Z in the epigenetic modulation of chromatin in this organism. Further research on how chromatin, chromosome maintenance, DNA integrity, DNA replication, and gene expression are controlled in *T. gondii* could also provide insights into epigenetic regulation in other parasites of the phylum. This research may also offer a novel mechanism for regulating gene expression and chromatin structure in organisms with complex life cycles that are evolutionarily distant from fungi and vertebrates.

Materials and methods

Parasite culture and manipulation

RHΔ*hxgprt* strain was used in all cases and grown in standard tachyzoite conditions *in vitro*: hTERT (ATCC® CRL-4001, USA) monolayers were infected with tachyzoites and incubated with Dulbecco's modified Eagle medium (DMEM, Invitrogen) supplemented with 1% fetal bovine serum (FBS, Internegocios S.A., Argentina) and penicillin (10,000 units/ml)-streptomycin (10 mg/ml) solution (Gibco, Argentina) at 37°C and 5% CO_2.

Cloning over-expression strategy

To generate the c-Myc-H2B.Z WT construct, the open reading frame (ORF) was amplified using the primers F: 5'-ATGCATTCAGGGAAAGGTCCGGCACAG-3' and R: 5'-TTAATTAACTATGCACCAGAAGTCGTG-3'. For the mutant constructs, reverse primer was the same, and forward was: ATGCATTCAGGG**GCA**GGTCCGGCACAG**GCA**TCTCAGGCGGCG**GCGGCG**ACCGCCGGG**GCG**TCTCTGGGAC for c-Myc-A, ATGCATTCAGGG**CGC**GGTCCGGCACAG**CGC**TCTCAGGCGGCG**CGCCGC**ACCGCCGGG**CGC**TCTCTGGGAC for c-Myc-R, where lysine coding codons were replaced for alanine and arginine coding codons, respectively (in bold type). NsiI and PacI restriction sites (underlined) were engineered into the 5' end of primers F and R, respectively, to clone into *T. gondii* expression vector PTUB8mycGFPPfTailTy-HX (a kind gift of Dr. Dominique Soldati, Université de Geneve) with a strong tubulin promoter. The resulting PCR product of the expected size was removed using a Qiaex II Gel Extraction kit (Qiagen), cloned in pGEM-T vector (Promega) and sequenced (Macrogen). The cloned ORF was digested with NsiI and PacI and ligated into the plasmid. The final plasmids were electroporated into RH strain tachyzoites lacking hypoxanthine–xanthine guanine phosphoribosyl transferase (RHΔ*hxgprt*). Transgenic parasites were selected in mycophenolic acid (25 μg/ml, Sigma) and xanthine (50 μg/ml, Sigma) and cloned by limiting dilution.

CRISPR/Cas9 gene deletion strategy

Single guide RNAs were designed directed to the N-terminal portion of the *h2bz* gene: F: AAGTTGAGGCGGCGAAGAAGACCGCCG and R: AAAACGGCGGTCTTCTTCGCCGCCTCA. Bsa I restriction sites were included (underlined). Both oligos were annealed and cloned into the pU6 CRISPR Universal plasmid (kindly provided by Louridós Lab, Whitehead Institute), by using the Bsa I restriction site. The plasmids were confirmed by PCR, using the gRNA as primers, were sequenced (Macrogen) and prepared for transfection in *Toxoplasma*. In order to obtain a clean KO, oligos were also designed to amplify the DHFR selection cassette from the pUPRT_DHFR

plasmid available in the laboratory, with homology regions (20 bp underlined) to the 3ánd 5ÚTR of the *h2bz* gene (F: GAAAGGTCCGGCACAGAAATCTCAGGCGGCGAAGAAGACCAAGCTTCGCCAGGC TGTAAATCC, and R: GAATTCCCTCTCAACATCAAATTTCACCCCGTGGTTTATTCCTCATCCTGCAAGTG CATAGAAGGA). The PCR amplification product was purified from agarose gel and used to co-transfect the parasites along with the CRISPR plasmid. c-Myc-R and c-Myc-A tachyzoites (one clone for each one was selected) were transfected and Pyrimethamine (1 μm, Sigma) was used for selection. Cas9 was detected in the nucleus of the parasites after transfection by using α-Flag antibody (Sigma, F1804). Selection was continued until three passages and cloning by limiting dilution was performed. Positive clones were selected by PCR with primers designed for that purpose: TgH2Bv-upUTR-F: GTTGTCATGCGCATTTGCATCAC; TgH2Bv-downUTR-R: GTGTGCACGCGTTATAATGAGCAC; Val-TgH2Bv-R: CATGCTCTTCTTCGACACACCAG; DHFRCX-F: GTGGCATTTCACACAGTCTCACCTC; DHFRCX-R: AGACGCAGACGCATACAACGTTAG.

Immunofluorescence assay (IFA)

Intracellular tachyzoites grown in cover slips were fixed using cold methanol 100% for 8 min, washed with PBS and blocked with 1% BSA. Primary antibody α-rH2B.Z (rabbit), α-rSag1 (mouse), α-rHSP90 (rabbit), α–rROP5 (rabbit), α–rROP18 (rabbit) produced in the laboratory and α-c-Myc (rabbit, abCam ab9106 or mouse, Santa Cruz sc-42), α–AcTubulin (mouse, Millipore MABT868) were incubated for 1 h at room temperature. After several washes with PBS cover slips were incubated with secondary antibodies Alexa fluor goat anti-mouse 488 and anti-rabbit 594 (Invitrogen). DAPI was used to stain nuclei. Axio Imager.M2 Microscope Carl Zeiss (Germany) with objective Plan-Apochromat 63x/1.40 Oil M27 and Video digital camera Zeiss 503 monochromatic 2.8 megapixeles, was used. Image J 1.53q (Fiji) software was used to process images.

Western blot analysis

Tachyzoites were collected, filtered, counted and lysed by 6 cycles of rapid freezing/defreeze in hypotonic buffer, and boiled with LB for 5 minutes. 0.5 to 1×10^7 parasites were loaded per well and resolved by 15% SDS-PAGE. Proteins were transferred to PVDF membrane for 1h at 100V. Western blot was then performed as described [90]. The primary antibodies: α-rH2B.Z [22], α-rH2A.Z [23], α–rROP5 (rabbit) and α–rROP18 (rabbit) were used at 1/5000, whereas α-c-Myc (rabbit, abCam ab9106) was used at 1/2000 and α-rSag1 [87] 1/200 for 1 h at room temperature. α-H3ac (rabbit, Millipore, 06–599B) 1/200, was incubated overnight. Appropriate secondary antibodies were used: phosphatase alkaline-conjugated goat anti-mouse or anti-rabbit (Sigma) along with the NBT and BCIP (Promega) detection system.

Phenotypical assays

For growth/competition assays, coverslips seeded with Htert cells were infected with a mix of 50% parental (RHΔ*hxgprt*) and 50% of each clone. 3 coverslips per clone were infected

with 0,05 to 0,1 tachyzoite per cell, incubated 10 minutes on ice, and 2 hours at 37°C in incubator for invasion. Slides were washed twice with PBS to remove tachyzoites that did not enter the cells, and fresh DMEM supplemented with 1% SFB was added. Slides were fixed at different times, up to 96 hours and IFA was performed with α-c-Myc and α-Sag1 antibodies to distinguish between parental and c-Myc positive vacuoles. Number of c-Myc positive and total vacuoles in at least 100 vacuoles, randomly choosing different fields of each slide were counted. In the case of competition assays with genotoxic drugs treatment, the experiment was modified as follows: 3 slides per clone mixture were fixed after 24 h, to stablish the initial percentage of c-Myc positive vacuoles. At this time point, media was changed in the rest of the slides for DMEM supplemented with DMSO or drugs at the concentrations indicated. These slides were fixed after 96 h, and IFA was performed and counted as explained before.

For *in vitro* differentiation assays, in a similar way using Htert confluent slides, media was changed by DMEM HEPES pH 8.1, after invasion with 1 parasite every 10 cells, accompanied with deprivation of CO_2. Media was changed every day, and differentiation rate was estimated after 96 h by using *Dolichos Biflorus* Lectin conjugated to Fluorescein (DLB 1:200, FL-1031; Vector Laboratories) to stain the wall of the cysts in formation and α-Sag1 antibody to stain the tachyzoites. In the case of collection of parasites for RNA extraction, differentiation assay was performed in a similar way, but in t25 dishes. After 48 or 96 h parasites were forced out of the cells by 23G, 25G and 27G syringe passages.

For *in vivo* survival, virulence and differentiation assays, C57BL/6 female mice were used. For the use of animals, C.I.C.U.A.E-UNSAM 10/22 was approved. Mice were maintained in optimal conditions in the biotherium, with controlled temperature and free access to sterilized water and food. Infection was carried out intra-peritoneal in 10 mice per group with 100, 1000 or 10000 tachyzoites of parental lines or clones, depending on the assay. PBS was injected as negative control in five mice per experiment. Deceases were registered along 30–35 days in each experiment, and signs of illness were monitored daily. Two mice from each group (except PBS) were sacrificed at day 5 (when RH infected mice have symptoms of illness), and intraperitoneal fluids were collected in order to detect acute *Toxoplasma* infection. Blood samples were taken at days 0, 14, 21 and 35 and sera was frozen for ELISA assays. After sacrifice, surviving mice brains were processed for cyst observance by optical microscopy. Also, a sample was stained using DLB and checked by fluorescence microscopy.

In every phenotypical assay, three independent experiments were performed. One representative experiment is shown.

RT-PCR and RT-qPCR

Tachyzoites or parasites exposed to 48 or 96 h differentiation stress as explained before were conserved in TriZol (Invitrogen) solution at −80°C until use. All experiments were performed in three independent replicates. RNA extraction was performed according to the manufacturer's instructions and cDNA was obtained by means of MMLV reverse transcriptase (Promega) using oligo dT with the protocol provided with the enzyme. For RT-PCR, primers used were: SAG1: Fw: TGAGAACCCGTGGCAGGGTAA;

Rv: GCTTTTTGACTCGGCTGGAA; TUB: Fw: ATGTTCCGTGGTCGCATGT; Rv: TGGGAATCCACTCAACGAAGT; ACTIN: Fw: GGGCGGTTTCATGACCTAAA; Rv: ACGTATGATGCGCGAGAAAA; ROP5: Fw: CTAGCTAGCATGGCGACGAAGCTCG; Rv: CCCAAGCTTTCAAGCGACTGAGGGCGCA; ROP18: Fw: CTAGCTAGCATGTTTTCGGTACAGCGGCCA; Rv: GCCAAGCTTTTATTCTGTGTGGAGATGTTC.

For RT-qPCR primers used were: SAG1: Fw: TGAGAACCCGTGGCAGGGTAA; Rv: GCTTTTTGACTCGGCTGGAA; BAG1: Fw: CAACGGAGCCATCGTTATCAAAGG; Rv: TAGAACGCCGTTGTCCATTG; LDH2: Fw: ACAATGGCCCAGGCATTCT; Rv: CAATAAACATATCGTGAAGCCCATA; AP2IX-9: Fw: GGGCGTTCTCAGCGTTCACT; Rv: GGCGCGTCTCATCTGTTTCA; AP2IV-3: Fw: GAGCCCATTGACCCCATGAA; Rv: GGCTTCGCTTCTTTCCGTGA; BFD1: Fw: ATGTCGGGAACGATGGTTTA; Rv: TCTTCACGGCATTCTCTGTG; TUB: Fw: ATGTTCCGTGGTCGCATGT; Rv: TGGGAATCCACTCAACGAAGT; ACTIN: Fw: GGGCGGTTTCATGACCTAAA; Rv: ACGTATGATGCGCGAGAAAA.

The primers were first assayed for efficiency using a pooled cDNA in 1 to 0.001 dilutions, and the threshold was defined for each set of primers. Melt curves were also obtained for each set. For each set of experiments, SybrGreen master solution (Roche) was used and qPCR was run in StepOne Real time equipment (Applied Biosystems). Actin and tubulin were used as housekeeping genes and data was normalized to those genes by Infostat software. For the experiments in figure 3, all sets of data were relativized to tachyzoite amplification. For experiment shown in figure 7, data from the different clones was relativized to the parental.

ELISA assay

Blood samples were extracted from surviving mice at days 0 (Pi), 14, 21 and 35. Sera was frozen until processing for ELISA. TLA (Toxoplasma lysate antigen, obtained from fresh RH tachyzoites) in buffer Carbonate (7,13g/L NaHCO3 + 1,59 g/L Na2CO3 pH 9,5) was used to immobilize 96 well plaques (Nunc Immuno™ MicroWell™ 96 well solid plates, Sigma), o.n. at 4°C. After bocking with 5% non-fat milk in PBS-T they were incubated with sera diluted 1:100 in the same solution. Total IgG (IgGt) and subtypes (IgG1, IgG2a and IgG2b) HRP-conjugated anti-mouse, made in rat, were used 1:5000. Tetramethyl-bencidine (TMB, Invitrogen) was used to reveal, and plaques were read after 20 min reaction at 655 nm in a Synergy H1. Data was analyzed in GraphPad Prism v7. Sera from mice inoculated with PBS (negative control) or infected with Me49 (positive control) were assayed.

Co-Immunoprecipitation (Co-IP)

Approximately 5×10^8 RHΔ*hxgprt* tachyzoites were used for each immunoprecipitation. Tachyzoites were treated with micrococcal endonuclease (MNase) in order to obtain mononucleosomes as described [23] and Co-IP was performed as described in Dalmasso et al [23] with minor modifications. Protease inhibitor cocktail (Sigma) was added in every step. Mononucleosomes were incubated with Agarose c-Myc beads (abCam, ab1253) overnight at 4°C. Alternatively, protein A/G Plus-agarose (sc-2003, Santa Cruz) incubated

for two hours with α-rH2B.Z (50 μl) or pre-immune sera was used. Immunocomplexes were washed twice with washing buffer 1 (50 mM Tris, pH8, 200 mM NaCl and 0.05 % Igepal100), twice with washing buffer 2 (50 mM Tris, pH8, 300 mM NaCl and 0.05 % Igepal100), and twice with buffer TE (10 mM Tris, pH8, 1 mM EDTA); then resuspended in 60 μl of SDS-PAGE loading buffer. Samples were boiled for 5 min and 20 μl were loaded per well in a 15% SDS-PAGE gel for immunoblotting. The absence of contaminating proteins was corroborated by western blot with murine α-SAG1 antibody [87]. Quantification of the bands was done with Image J 1.53q (Fiji) software.

Tachyzoites nuclei size assay

Three slides with confluent hTert cells were infected as explained before with parental or c-Myc-A/c-Myc-R/c-Myc-WT-OE clones and let replicate for 24 hours. Slides were fixed and IFA was performed as explained before using αrH2B.Z to stain nuclei. Images were processed with Image J 1.53q (Fiji) software to measure the size of the nuclei, by delimiting them with the appropriate tool in at least 50 vacuoles in fields randomly chosen, for each slide and each independent experiment. Data was graphed and statistical analyzed with GraphPad Prism 8 software.

Peptide synthesis and characterization

Peptides were synthesized by solid-phase multiple peptide system using tea-bags with Fmoc/tBu strategy according Guzmán [91], briefly: Rink amide resin (0.55 meq/g) was used as solid support and Fmoc amino acids, including acetylated lysine (Iris Biotech). Peptides were couplet to biotin for their detection The peptide cleavage was performed with a solution of Trifluoracetic acid/triisopropylsilane/1.2-ethandithiol /water (92.5 /2.5 /2.5/2.5), washed with cold ether dried and lyophilized. Peptides were characterized by HPLC and electrospray ionization mass spectrometry, and purified by C18 cartridges (United Chemical Technologies, Bristol, PA, USA) before use.

Peptides used in the pull-down assays were: Un-acetylated: GPAQKSQAAKKTAGKSLGPRK(Biotin)

Acetylated: GPAQKSQAAK(Ac)K(Ac)TAGKSLGPR-K(Biotin)

Pull-down assays

Pull-down experiments were performed as detailed in Wysocka [52] after nuclear extraction with NE-PER commercial kit following manufacturer's instructions (Thermo Scientific #78833) and run in SDS-PAGE for a short time in order to avoid separation. Protein gels were fixed by soaking for 3 hr in 30% methanol, 2% phosphoric acid. Then the gel was washed with deionized water 3 times, 5 minutes each. After removing the deionized water, the staining solution (0.5 g/L Coomasie blue brilliant R250, 18% methanol, 17% $(NH_4)2SO_4$, 2% phosphoric acid) was added until covering the gel. It was stained for 1 h in gentle shaking. Then the gel was rinsed in deionized water 3 times for 5 minutes each. The background staining was removed with 30% methanol. The gel was stored in deionized water until use. Each lane of the gel was cut into individual slices. Each band was then cut into 1 mm^3 cube and further treated with three washes of 50 mM NH_4HCO_3 in 50% CH_3CN

with 10 min incubations. Each group of gel cubes was then dehydrated in CH_3CN for 10 min and dried in a Speed Vac. Protein samples were reduced by dithiothreitol (DTT) and alkylated by iodoacetamide [92]. A solution of 10 ng/μL trypsin in 50 mM NH_4HCO_3 was used to re-swell the gel pieces completely at 4°C for 30 min, followed by a 37°C digestion overnight. A small amount of 10% formic acid was then added to stop the digestion. The sample was then centrifuged at 2,800 x g, and the supernatant was collected for LC-MS/MS.

LC-MS/MS Analysis

A fused silica microcapillary LC column (15-cm long x 75-μm inside diameter) packed with Halo C18 reversed-phase resin (2.7 μm particle size, 90 nm pore size, MichromBioresources.) was used with EASY-nLC 1200 system (Thermo Fisher). The nanospray ESI was fitted onto the Thermo Q-Exactive plus mass spectrometer (Thermo Electron, San Jose, CA) that was operated in a Higher-energy C-trap dissociation mode to obtain both MS and tandem MS (MS/MS) spectra. Two μL of tryptic peptide samples were loaded onto the microcapillary column and separated by applying a gradient of 3–40% acetonitrile in 0.1% formic acid at a flow rate of 300 nL/min for 80 min. Mass spectrometry data were acquired in a data-dependent top-10 acquisition mode, which uses a full MS scan from m/z 350–1700 at 70,000 resolution (automatic gain control [AGC] target, 1e6; maximum ion time [max IT], 100 ms; profile mode). Resolution for dd-MS2 spectra was set to 17,500 (AGC target: 1e5) with a maximum ion injection time of 50 ms. The normalized collision energy was 27 eV.

Protein Identification

Obtained MS spectra were searched against the *T. gondii* ToxoDB-42 _TgondiiME49 protein database using Proteome Discoverer 2.2 (Thermo Electron, San Jose, CA). The search parameters permitted a 10 ppm peptide MS tolerance and a 0.02 Da MS/MS tolerance. Carboxymethylation of cysteines was set as a fixed modification, and oxidation of methionine as a dynamic modification. Up to two missed tryptic peptide cleavages were considered. The proteins for which the False Discovery Rate was less than 1% at the peptide level were included in the following analysis. The raw data of all mass spectra had been submitted to the MassIVE (https://massive.ucsd.edu/; Project accession: MassIVE MSV000091226).

Supplementary Material

Refer to Web version on PubMed Central for supplementary material.

Acknowledgments:

L. Vanagas (Researcher), D. Muñoz (Fellow), C. Cristaldi (Fellow), D. Ganuza (Technician), V. Turowski (Researcher), and S.O. Angel (Researcher) are members of CONICET. S.O. Angel (Full) and L. Vanagas (Adjunct) are Professors at Universidad Nacional General de San Martin (UNSAM). The Vermont Biomedical Research Network (VBRN) Proteomics Facility is supported through NIH grant P20GM103449 from the INBRE Program of the National Institute of General Medical Science (BD).

Funding:

This work was supported by the Ministerio Nacional de Ciencia y Tecnología (MINCyT): PICT 2015 1288 (S.O.A.), PICT 2018 2434 (L.V.), Consejo Nacional de Investigaciones Científicas y Tecnológicas (CONICET): PIP 11220150100145CO and 11220210100572CO (S.O.A., L.V.) and by National Institute of Health: NIH-NIAID 1R01AI129807 (S.O.A.) and AI152583 (to W.J.S.).

Data Availability Statement:

The data that support the findings of this study are available from the corresponding author upon reasonable request.

References

[1]. Vanagas L, Jeffers V, Bogado SS, Dalmasso MC, Sullivan WJ Jr., Angel SO Toxoplasma histone acetylation remodelers as novel drug targets. Expert review of anti-infective therapy. 2012;10:1189–201. [PubMed: 23199404]

[2]. Mouveaux T, Rotili D, Boissavy T, Roger E, Pierrot C, Mai A, et al. A potent HDAC inhibitor blocks Toxoplasma gondii tachyzoite growth and profoundly disrupts parasite gene expression. Int J Antimicrob Agents. 2022;59:106526.

[3]. Kim K The Epigenome, Cell Cycle, and Development in Toxoplasma. Annual review of microbiology. 2018;72:479–99.

[4]. Pappas G, Roussos N, Falagas ME. Toxoplasmosis snapshots: global status of Toxoplasma gondii seroprevalence and implications for pregnancy and congenital toxoplasmosis. Int J Parasitol. 2009;39:1385–94. [PubMed: 19433092]

[5]. Attias M, Teixeira DE, Benchimol M, Vommaro RC, Crepaldi PH, De Souza W. The life-cycle of Toxoplasma gondii reviewed using animations. Parasit Vectors. 2020;13:588. [PubMed: 33228743]

[6]. Weiss LM, Kim K. The development and biology of bradyzoites of Toxoplasma gondii. Front Biosci. 2000;5:D391–405. [PubMed: 10762601]

[7]. Luft BJ, Remington JS. Toxoplasmic encephalitis in AIDS. Clin Infect Dis. 1992;15:211–22. [PubMed: 1520757]

[8]. Carlier Y, Truyens C, Deloron P, Peyron F. Congenital parasitic infections: a review. Acta Trop. 2012;121:55–70. [PubMed: 22085916]

[9]. Brynska A, Tomaszewicz-Libudzic E, Wolanczyk T. Obsessive-compulsive disorder and acquired toxoplasmosis in two children. Eur Child Adolesc Psychiatry. 2001;10:200–4. [PubMed: 11596821]

[10]. Miman O, Mutlu EA, Ozcan O, Atambay M, Karlidag R, Unal S. Is there any role of Toxoplasma gondii in the etiology of obsessive-compulsive disorder? Psychiatry Res. 2010;177:263–5. [PubMed: 20106536]

[11]. Yolken RH, Dickerson FB, Fuller Torrey E. Toxoplasma and schizophrenia. Parasite Immunol. 2009;31:706–15. [PubMed: 19825110]

[12]. Vittecoq M, Elguero E, Lafferty KD, Roche B, Brodeur J, Gauthier-Clerc M, et al. Brain cancer mortality rates increase with Toxoplasma gondii seroprevalence in France. Infect Genet Evol. 2012;12:496–8. [PubMed: 22285308]

[13]. de Haan L, Sutterland AL, Schotborgh JV, Schirmbeck F, de Haan L. Association of Toxoplasma gondii Seropositivity With Cognitive Function in Healthy People: A Systematic Review and Meta-analysis. JAMA Psychiatry. 2021;78:1103–12. [PubMed: 34259822]

[14]. Waldman BS, Schwarz D, Wadsworth MH 2nd, Saeij JP, Shalek AK, Lourido S Identification of a Master Regulator of Differentiation in Toxoplasma. Cell. 2020;180:359–72 e16. [PubMed: 31955846]

[15]. Jeffers V, Tampaki Z, Kim K, Sullivan WJ Jr. A latent ability to persist: differentiation in Toxoplasma gondii. Cellular and molecular life sciences : CMLS. 2018;75:2355–73. [PubMed: 29602951]

[16]. Bougdour A, Maubon D, Baldacci P, Ortet P, Bastien O, Bouillon A, et al. Drug inhibition of HDAC3 and epigenetic control of differentiation in Apicomplexa parasites. The Journal of experimental medicine. 2009;206:953–66. [PubMed: 19349466]

[17]. Nardelli SC, Silmon de Monerri NC, Vanagas L, Wang X, Tampaki Z, Sullivan WJ Jr., et al. Genome-wide localization of histone variants in Toxoplasma gondii implicates variant exchange in stage-specific gene expression. BMC genomics. 2022;23:128. [PubMed: 35164683]

[18]. Santisteban MS, Kalashnikova T, Smith MM. Histone H2A.Z regulats transcription and is partially redundant with nucleosome remodeling complexes. Cell. 2000;103:411–22. [PubMed: 11081628]

[19]. Oberdoerffer P, Miller KM. Histone H2A variants: Diversifying chromatin to ensure genome integrity. Semin Cell Dev Biol. 2022.

[20]. Xu Y, Ayrapetov MK, Xu C, Gursoy-Yuzugullu O, Hu Y, Price BD. Histone H2A.Z controls a critical chromatin remodeling step required for DNA double-strand break repair. Mol Cell. 2012;48:723–33. [PubMed: 23122415]

[21]. Fenoy IM, Bogado SS, Contreras SM, Gottifredi V, Angel SO. The Knowns Unknowns: Exploring the Homologous Recombination Repair Pathway in Toxoplasma gondii. Front Microbiol. 2016;7:627. [PubMed: 27199954]

[22]. Dalmasso MC, Echeverria PC, Zappia MP, Hellman U, Dubremetz JF, Angel SO. Toxoplasma gondii has two lineages of histones 2b (H2B) with different expression profiles. Molecular and biochemical parasitology. 2006;148:103–7. [PubMed: 16621068]

[23]. Dalmasso MC, Onyango DO, Naguleswaran A, Sullivan WJ Jr., Angel SO Toxoplasma H2A variants reveal novel insights into nucleosome composition and functions for this histone family. J Mol Biol. 2009;392:33–47. [PubMed: 19607843]

[24]. Dalmasso MC, Sullivan WJ Jr., Angel SO Canonical and variant histones of protozoan parasites. Frontiers in bioscience. 2011;16:2086–105.

[25]. Petter M, Selvarajah SA, Lee CC, Chin WH, Gupta AP, Bozdech Z, et al. H2A.Z and H2B.Z double-variant nucleosomes define intergenic regions and dynamically occupy var gene promoters in the malaria parasite Plasmodium falciparum. Molecular microbiology. 2013;87:1167–82. [PubMed: 23373537]

[26]. Lowell JE, Kaiser F, Janzen CJ, Cross GA. Histone H2AZ dimerizes with a novel variant H2B and is enriched at repetitive DNA in Trypanosoma brucei. J Cell Sci. 2005;118:5721–30. [PubMed: 16303849]

[27]. Sidik SM, Huet D, Ganesan SM, Huynh MH, Wang T, Nasamu AS, et al. A Genome-wide CRISPR Screen in Toxoplasma Identifies Essential Apicomplexan Genes. Cell. 2016;166:1423–35 e12. [PubMed: 27594426]

[28]. Nardelli SC, Che FY, Silmon de Monerri NC, Xiao H, Nieves E, Madrid-Aliste C, et al. The histone code of Toxoplasma gondii comprises conserved and unique posttranslational modifications. mBio. 2013;4:e00922–13. [PubMed: 24327343]

[29]. Giaimo BD, Ferrante F, Herchenrother A, Hake SB, Borggrefe T. The histone variant H2A.Z in gene regulation. Epigenetics & chromatin. 2019;12:37. [PubMed: 31200754]

[30]. Talbert PB, Henikoff S. Histone variants--ancient wrap artists of the epigenome. Nature reviews Molecular cell biology. 2010;11:264–75. [PubMed: 20197778]

[31]. Bruce K, Myers FA, Mantouvalou E, Lefevre P, Greaves I, Bonifer C, et al. The replacement histone H2A.Z in a hyperacetylated form is a feature of active genes in the chicken. Nucleic Acids Res. 2005;33:5633–9. [PubMed: 16204459]

[32]. Binda O, Sevilla A, LeRoy G, Lemischka IR, Garcia BA, Richard S. SETD6 monomethylates H2AZ on lysine 7 and is required for the maintenance of embryonic stem cell self-renewal. Epigenetics. 2013;8:177–83. [PubMed: 23324626]

[33]. Law C, Cheung P. Expression of Non-acetylatable H2A.Z in Myoblast Cells Blocks Myoblast Differentiation through Disruption of MyoD Expression. J Biol Chem. 2015;290:13234–49. [PubMed: 25839232]

[34]. Valdes-Mora F, Song JZ, Statham AL, Strbenac D, Robinson MD, Nair SS, et al. Acetylation of H2A.Z is a key epigenetic modification associated with gene deregulation and epigenetic remodeling in cancer. Genome research. 2012;22:307–21. [PubMed: 21788347]

[35]. Whittle CM, McClinic KN, Ercan S, Zhang X, Green RD, Kelly WG, et al. The genomic distribution and function of histone variant HTZ-1 during C. elegans embryogenesis. PLoS Genet. 2008;4:e1000187.

[36]. Updike DL, Mango SE. Temporal regulation of foregut development by HTZ-1/H2A.Z and PHA4/FoxA. PLoS Genet. 2006;2:e161. [PubMed: 17009877]

[37]. Ridgway P, Brown KD, Rangasamy D, Svensson U, Tremethick DJ. Unique residues on the H2A.Z containing nucleosome surface are important for Xenopus laevis development. J Biol Chem. 2004;279:43815–20. [PubMed: 15299007]

[38]. Myers FA, Chong W, Evans DR, Thorne AW, Crane-Robinson C. Acetylation of histone H2B mirrors that of H4 and H3 at the chicken beta-globin locus but not at housekeeping genes. J Biol Chem. 2003;278:36315–22. [PubMed: 12865423]

[39]. Miao J, Fan Q, Cui L, Li J, Li J, Cui L. The malaria parasite Plasmodium falciparum histones: organization, expression, and acetylation. Gene. 2006;369:53–65. [PubMed: 16410041]

[40]. Trelle MB, Salcedo-Amaya AM, Cohen AM, Stunnenberg HG, Jensen ON. Global histone analysis by mass spectrometry reveals a high content of acetylated lysine residues in the malaria parasite Plasmodium falciparum. Journal of proteome research. 2009;8:3439–50. [PubMed: 19351122]

[41]. Radke JB, Lucas O, De Silva EK, Ma Y, Sullivan WJ Jr., Weiss LM, et al. ApiAP2 transcription factor restricts development of the Toxoplasma tissue cyst. Proc Natl Acad Sci U S A. 2013;110:6871–6. [PubMed: 23572590]

[42]. Hong DP, Radke JB, White MW. Opposing Transcriptional Mechanisms Regulate Toxoplasma Development. mSphere. 2017;2.

[43]. Gursoy-Yuzugullu O, Ayrapetov MK, Price BD. Histone chaperone Anp32e removes H2A.Z from DNA double-strand breaks and promotes nucleosome reorganization and DNA repair. Proc Natl Acad Sci U S A. 2015;112:7507–12. [PubMed: 26034280]

[44]. Morillo-Huesca M, Clemente-Ruiz M, Andujar E, Prado F. The SWR1 histone replacement complex causes genetic instability and genome-wide transcription misregulation in the absence of H2A.Z. PloS one. 2010;5:e12143.

[45]. Munera Lopez J, Ganuza A, Bogado SS, Munoz D, Ruiz DM, Sullivan WJ Jr., et al. Evaluation of ATM Kinase Inhibitor KU-55933 as Potential Anti-Toxoplasma gondii Agent. Frontiers in cellular and infection microbiology. 2019;9:26. [PubMed: 30815397]

[46]. Angel SO, Vanagas L, Ruiz DM, Cristaldi C, Saldarriaga Cartagena AM, Sullivan WJJ. Emerging Therapeutic Targets Against Toxoplasma gondii: Update on DNA Repair Response Inhibitors and Genotoxic Drugs. Front Cell Infect Microbiol. 2020;10.

[47]. Behnke MS, Fentress SJ, Mashayekhi M, Li LX, Taylor GA, Sibley LD. The polymorphic pseudokinase ROP5 controls virulence in Toxoplasma gondii by regulating the active kinase ROP18. PLoS pathogens. 2012;8:e1002992.

[48]. Etheridge RD, Alaganan A, Tang K, Lou HJ, Turk BE, Sibley LD. The Toxoplasma pseudokinase ROP5 forms complexes with ROP18 and ROP17 kinases that synergize to control acute virulence in mice. Cell host & microbe. 2014;15:537–50. [PubMed: 24832449]

[49]. Reese ML, Zeiner GM, Saeij JP, Boothroyd JC, Boyle JP. Polymorphic family of injected pseudokinases is paramount in Toxoplasma virulence. Proc Natl Acad Sci U S A. 2011;108:9625–30. [PubMed: 21436047]

[50]. Saeij JP, Boyle JP, Coller S, Taylor S, Sibley LD, Brooke-Powell ET, et al. Polymorphic secreted kinases are key virulence factors in toxoplasmosis. Science. 2006;314:1780–3. [PubMed: 17170306]

[51]. Fentress SJ, Behnke MS, Dunay IR, Mashayekhi M, Rommereim LM, Fox BA, et al. Phosphorylation of immunity-related GTPases by a Toxoplasma gondii-secreted kinase promotes macrophage survival and virulence. Cell host & microbe. 2010;8:484–95. [PubMed: 21147463]

[52]. Wysocka J Identifying novel proteins recognizing histone modifications using peptide pulldown assay. Methods. 2006;40:339–43. [PubMed: 17101446]

[53]. Attar N, Campos OA, Vogelauer M, Cheng C, Xue Y, Schmollinger S, et al. The histone H3-H4 tetramer is a copper reductase enzyme. Science. 2020;369:59–64. [PubMed: 32631887]

[54]. Singh A, Verma S, Modak SB, Chaturvedi MM, Purohit JS. Extra-nuclear histones: origin, significance and perspectives. Mol Cell Biochem. 2022;477:507–24. [PubMed: 34796445]

[55]. Choi YS, Hoon Jeong J, Min HK, Jung HJ, Hwang D, Lee SW, et al. Shot-gun proteomic analysis of mitochondrial D-loop DNA binding proteins: identification of mitochondrial histones. Molecular bioSystems. 2011;7:1523–36. [PubMed: 21359316]

[56]. Zanin MK, Donohue JM, Everitt BA. Evidence that core histone H3 is targeted to the mitochondria in Brassica oleracea. Cell Biol Int. 2010;34:997–1003. [PubMed: 20597863]

[57]. Roson JN, Vitarelli MO, Costa-Silva HM, Pereira KS, Pires DDS, Lopes LS, et al. H2B.V demarcates divergent strand-switch regions, some tDNA loci, and genome compartments in Trypanosoma cruzi and affects parasite differentiation and host cell invasion. PLoS pathogens. 2022;18:e1009694.

[58]. Croken MM, Nardelli SC, Kim K. Chromatin modifications, epigenetics, and how protozoan parasites regulate their lives. Trends Parasitol. 2012;28:202–13. [PubMed: 22480826]

[59]. Croken MM, Qiu W, White MW, Kim K. Gene Set Enrichment Analysis (GSEA) of Toxoplasma gondii expression datasets links cell cycle progression and the bradyzoite developmental program. BMC genomics. 2014;15:515. [PubMed: 24962434]

[60]. Wang J, Dixon SE, Ting LM, Liu TK, Jeffers V, Croken MM, et al. Lysine acetyltransferase GCN5b interacts with AP2 factors and is required for Toxoplasma gondii proliferation. PLoS pathogens. 2014;10:e1003830.

[61]. Jeffers V, Gao H, Checkley LA, Liu Y, Ferdig MT, Sullivan WJ Jr. Garcinol Inhibits GCN5Mediated Lysine Acetyltransferase Activity and Prevents Replication of the Parasite Toxoplasma gondii. Antimicrobial agents and chemotherapy. 2016;60:2164–70. [PubMed: 26810649]

[62]. Huang S, Holmes MJ, Radke JB, Hong DP, Liu TK, White MW, et al. Toxoplasma gondii AP2IX-4 Regulates Gene Expression during Bradyzoite Development. mSphere. 2017;2.

[63]. Khelifa AS, Guillen Sanchez C, Lesage KM, Huot L, Mouveaux T, Pericard P, et al. TgAP2IX-5 is a key transcriptional regulator of the asexual cell cycle division in Toxoplasma gondii. Nature communications. 2021;12:116.

[64]. Sindikubwabo F, Ding S, Hussain T, Ortet P, Barakat M, Baumgarten S, et al. Modifications at K31 on the lateral surface of histone H4 contribute to genome structure and expression in apicomplexan parasites. eLife. 2017;6.

[65]. Gissot M, Kelly KA, Ajioka JW, Greally JM, Kim K. Epigenomic modifications predict active promoters and gene structure in Toxoplasma gondii. PLoS pathogens. 2007;3:e77. [PubMed: 17559302]

[66]. Ren Q, Gorovsky MA. Histone H2A.Z acetylation modulates an essential charge patch. Mol Cell. 2001;7:1329–35. [PubMed: 11430834]

[67]. Ren Q, Gorovsky MA. The nonessential H2A N-terminal tail can function as an essential charge patch on the H2A.Z variant N-terminal tail. Mol Cell Biol. 2003;23:2778–89. [PubMed: 12665578]

[68]. Macadangdang BR, Oberai A, Spektor T, Campos OA, Sheng F, Carey MF, et al. Evolution of histone 2A for chromatin compaction in eukaryotes. eLife. 2014;3.

[69]. Severo V, Souza R, Vitorino F, Cunha J, Avila A, Arrizabalaga G, et al. Previously Unidentified Histone H1-Like Protein Is Involved in Cell Division and Ribosome Biosynthesis in Toxoplasma gondii. mSphere. 2022;7:e0040322.

[70]. SMR Sarah Sokol Borrelli, Sharp Katherine G., Cabo Leah F., Alrubaye Hisham S., Di Genova Bruno Martorelli and Boyle Jon P.. A transcriptional network required for Toxoplasma gondii tissue cyst formation is dispensable for long-term persistence. bioRxiv. 2022.

[71]. CJG M. Haley Licon, Sundeep Chakladar, Lindsey Shallberg, Waldman Benjamin S., Hunter Christopher A., Lourido Sebastian. A positive feedback loop controls Toxoplasma chronic differentiation. Biorxvi. 2022.

[72]. Colino-Sanguino Y, Cornett EM, Moulder D, Smith GC, Hrit J, Cordeiro-Spinetti E, et al. A Read/Write Mechanism Connects p300 Bromodomain Function to H2A.Z Acetylation. iScience. 2019;21:773–88. [PubMed: 31727574]

[73]. Afroz T, Cienikova Z, Clery A, Allain FHT. One, Two, Three, Four! How Multiple RRMs Read the Genome Sequence. Methods in enzymology. 2015;558:235–78. [PubMed: 26068744]

[74]. Malumbres M Cyclin-dependent kinases. Genome biology. 2014;15:122. [PubMed: 25180339]

[75]. Jin C, Zang C, Wei G, Cui K, Peng W, Zhao K, et al. H3.3/H2A.Z double variant-containing nucleosomes mark 'nucleosome-free regions' of active promoters and other regulatory regions. Nature genetics. 2009;41:941–5. [PubMed: 19633671]

[76]. Rahal R, Amon A. Mitotic CDKs control the metaphase-anaphase transition and trigger spindle elongation. Genes & development. 2008;22:1534–48. [PubMed: 18519644]

[77]. Lukasik P, Zaluski M, Gutowska I. Cyclin-Dependent Kinases (CDK) and Their Role in Diseases Development-Review. International journal of molecular sciences. 2021;22.

[78]. Ors A, Papin C, Favier B, Roulland Y, Dalkara D, Ozturk M, et al. Histone H3.3 regulates mitotic progression in mouse embryonic fibroblasts. Biochemistry and cell biology = Biochimie et biologie cellulaire. 2017;95:491–9. [PubMed: 28177753]

[79]. Page MJ, Di Cera E. Evolution of peptidase diversity. J Biol Chem. 2008;283:30010–4. [PubMed: 18768474]

[80]. Harvey SH, Krien MJ, O'Connell MJ. Structural maintenance of chromosomes (SMC) proteins, a family of conserved ATPases. Genome biology. 2002;3:REVIEWS3003.

[81]. Laflamme G, Tremblay-Boudreault T, Roy MA, Andersen P, Bonneil E, Atchia K, et al. Structural maintenance of chromosome (SMC) proteins link microtubule stability to genome integrity. J Biol Chem. 2014;289:27418–31. [PubMed: 25135640]

[82]. Serrano D, Cordero G, Kawamura R, Sverzhinsky A, Sarker M, Roy S, et al. The Smc5/6 Core Complex Is a Structure-Specific DNA Binding and Compacting Machine. Mol Cell. 2020;80:1025–38 e5. [PubMed: 33301731]

[83]. Borgogno MV, Monti MR, Zhao W, Sung P, Argarana CE, Pezza RJ. Tolerance of DNA Mismatches in Dmc1 Recombinase-mediated DNA Strand Exchange. J Biol Chem. 2016;291:4928–38. [PubMed: 26709229]

[84]. Denkers EY, Gazzinelli RT. Regulation and function of T-cell-mediated immunity during Toxoplasma gondii infection. Clin Microbiol Rev. 1998;11:569–88. [PubMed: 9767056]

[85]. Blader IJ, Saeij JP. Communication between Toxoplasma gondii and its host: impact on parasite growth, development, immune evasion, and virulence. APMIS. 2009;117:458–76. [PubMed: 19400868]

[86]. Elsaid MM, Vitor RW, Frezard FJ, Martins MS. Protection against toxoplasmosis in mice immunized with different antigens of Toxoplasma gondii incorporated into liposomes. Mem Inst Oswaldo Cruz. 1999;94:485–90. [PubMed: 10446006]

[87]. Sanchez-Lopez EF, Corigliano MG, Oliferuk S, Ramos-Duarte VA, Rivera M, Mendoza-Morales LF, et al. Oral Immunization With a Plant HSP90-SAG1 Fusion Protein Produced in Tobacco Elicits Strong Immune Responses and Reduces Cyst Number and Clinical Signs of Toxoplasmosis in Mice. Front Plant Sci. 2021;12:726910.

[88]. Buxton D, Innes EA. A commercial vaccine for ovine toxoplasmosis. Parasitology. 1995;110 Suppl:S11–6. [PubMed: 7784124]

[89]. Wu M, Liu S, Chen Y, Liu D, An R, Cai H, et al. Live-attenuated ME49Deltacdpk3 strain of Toxoplasma gondii protects against acute and chronic toxoplasmosis. NPJ Vaccines. 2022;7:98. [PubMed: 35986017]

[90]. Echeverria PC, Matrajt M, Harb OS, Zappia MP, Costas MA, Roos DS, et al. Toxoplasma gondii Hsp90 is a potential drug target whose expression and subcellular localization are developmentally regulated. J Mol Biol. 2005;350:723–34. [PubMed: 15967463]

[91]. Guzman F, Gauna A, Roman T, Luna O, Alvarez C, Pareja-Barrueto C, et al. Tea Bags for Fmoc Solid-Phase Peptide Synthesis: An Example of Circular Economy. Molecules. 2021;26.

[92]. Spiess PC, Deng B, Hondal RJ, Matthews DE, van der Vliet A. Proteomic profiling of acrolein adducts in human lung epithelial cells. J Proteomics. 2011;74:2380–94. [PubMed: 21704744]

Highlights:

- *Toxoplasma gondii* variant histone H2B.Z N-tail has 5 acetylatable lysines.
- We generated mutants where lysines were replaced by alanines or arginines (+ patch).
- Positive patch affects growth, differentiation, DNA damage response and virulence.
- Pull down with acetylated and non-acetylated peptides retrieved specific interactors.
- H2B.Z acetylation regulates a positive charge patch important for parasite fitness.

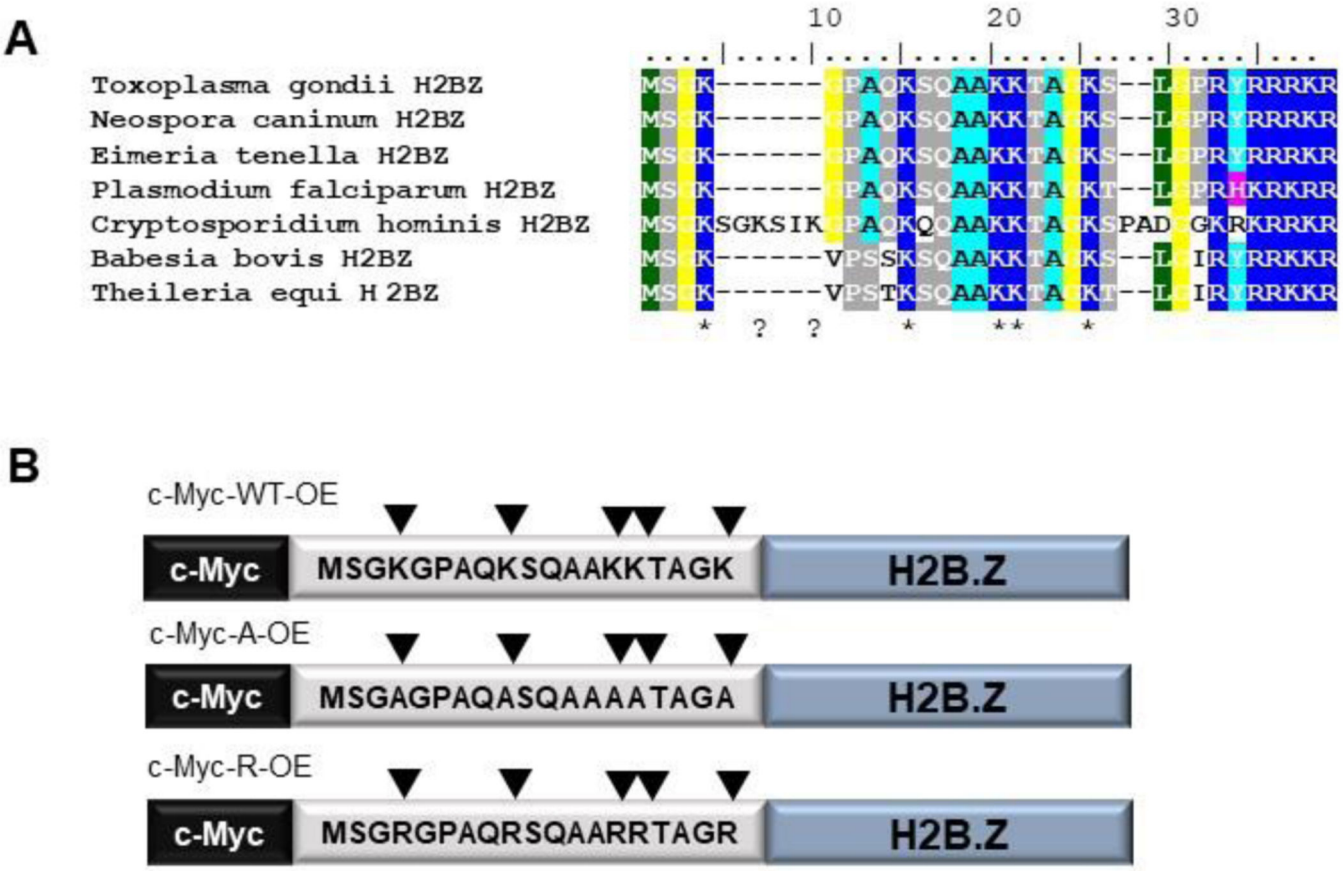

Figure 1. H2B.Z N-terminal tail acetylation and mutagenesis strategy.

A. Representative Apicomplexa H2B.Z N-terminal tail alignment. *Toxoplasma gondii* (TGME49_209910), *Neospora caninum* (NCLIV_004160), *Eimeria tenella* (ETH_00030960), *Plasmodium falciparum* (PF3D7_0714000.1), *Cryptosporidium hominis* (cgd7_1700-RA), *Babesia bovis* (BBOV_IV006840) and *Theileria equi* (BEWA_028110) H2B.Z protein sequences were aligned by Clustal W. The N-terminal tail region is shown. **B.** Schematic of the constructs generated in RHΔ*hxgprt* strain tachyzoites. The N-terminal region is shown with the amino acid sequence with or without mutations. All constructs were driven by the tubulin promoter, fused in-frame with a c-Myc epitope tag at the N-terminus.

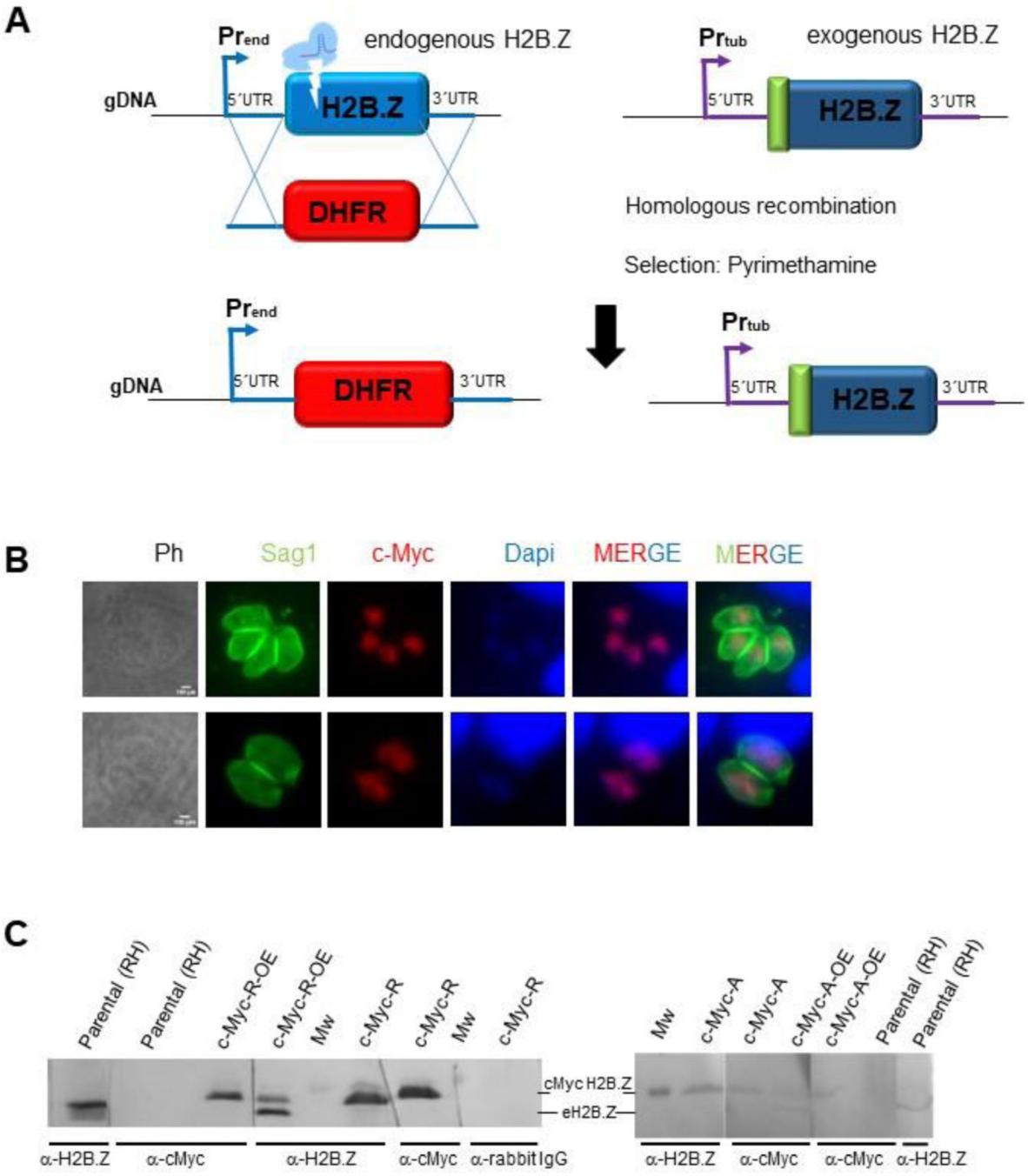

Figure 2. H2B.Z gene deletion strategy.

A. Schematic of CRISPR/Cas9-mediated deletion of endogenous *h2b.z*. Single guide RNA was directed to the N-terminal region of H2B.Z. Tachyzoites of c-Myc-R-OE and c-Myc-A-OE were co-transfected with Crispr plasmid and a PCR product obtained with primers to amplify DHFR selection cassette from a pUPRT_DHFR plasmid with homology arms (20 bp) to 5ánd 3ÚTR of *h2b.z*. The diagram shows the result after selection in pyrimethamine in which parasites have replaced endogenous *h2b.z* with the DHFR cassette, remaining c-Myc-H2B.Z sequence (with the corresponding mutations). gDNA: genomic DNA; Pr_{end}:

endogenous promoter; Pr_{tub}: tubulin promoter. **B.** Immunofluorescence assay: coverslips with confluent Htert cells were infected with 1 tachyzoite per cell of each designated clone and fixed after 18–24 hours. IFA was performed with α-cMyc (abCam), and α-Sag1 (mouse). α-IgG-mouse Alexa 488, and α-IgG rabbit Alexa 564 were applied 1:4,000 for 30 minutes. DAPI was used to stain nuclei. Scale bar=5 μm. **C.** Western blot of designated clones (0.5–1 $\times 10^7$ parasites per lane) proved with indicated antibodies: α-c-Myc, α-H2B.Z, secondary α-rabbit IgG (negative control). Overexpressing clones (c-Myc-R-OE and c-Myc-A-OE) used for transfection, as well as the parental (RH) were loaded as controls. Mw: molecular weight marker (17 kDa band). eH2B.Z: endogenous H2B.Z.

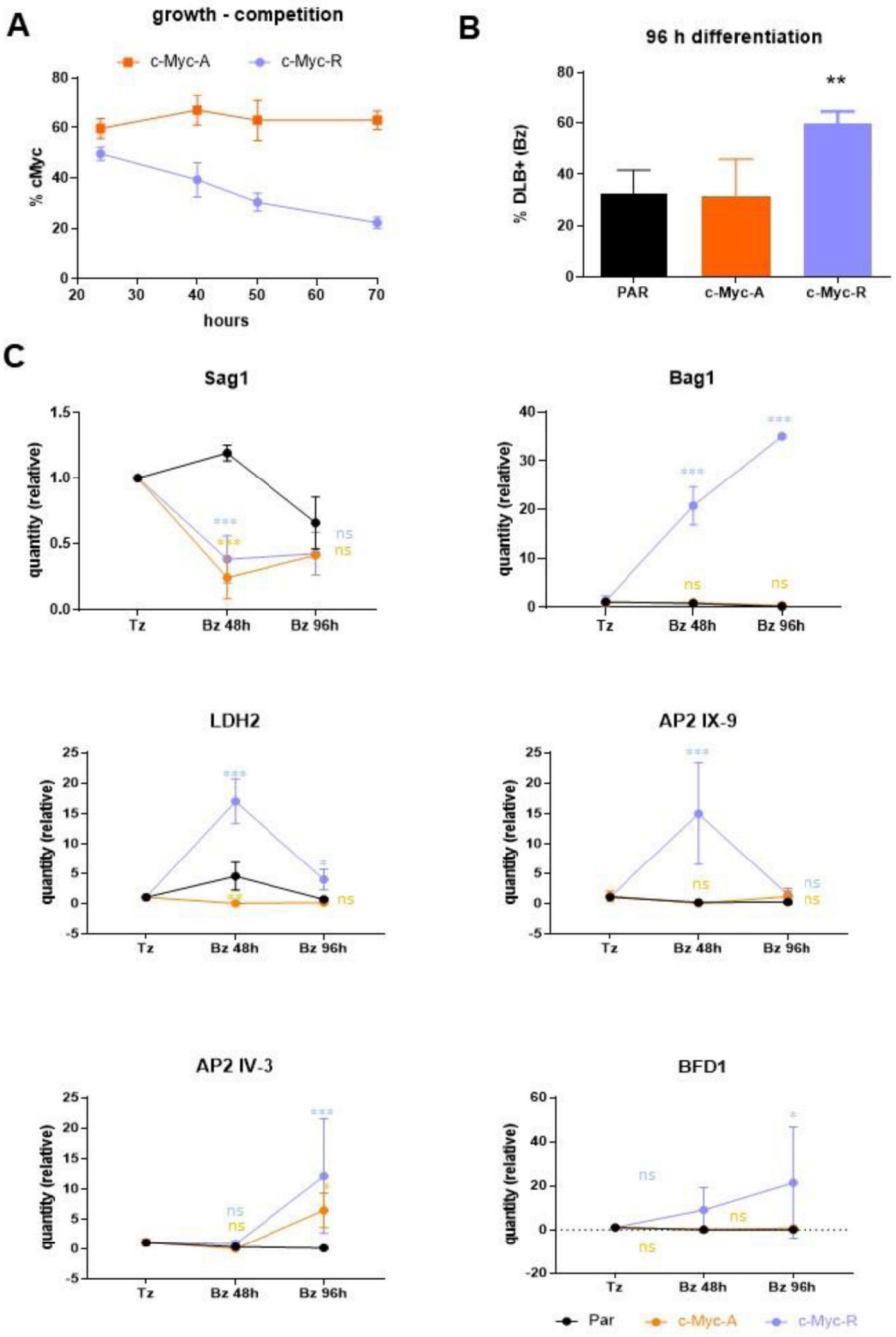

Figure 3. ***In vitro*** **growth and differentiation analysis on c-Myc-A and c-Myc-R.**

A. Growth assay with the percentage of c-Myc positive vacuoles expressed relative to the total (α-Sag1) from at least 100 vacuoles per slide. Three slides per clone were counted. Shown is a representative assay of three independent experiments. **B.** *In vitro* differentiation assay. Percentage of DLB-positive vacuoles was obtained after IFA with DLB (bradyzoites) and α-Sag1 (tachyzoites). Representative assay of three independent experiments. PAR: parental (RHΔ*hxgprt)*. Data was analyzed with Graphpad and one-way Anova was performed. **: $p < 0.01$. **C.** Tachyzoites (Tz) of parental (RHΔ*hxgprt*), c-Myc-

A or c-Myc-R were freshly collected and conserved in Trizol until processing. *In-vitro* differentiation was performed in dishes for 48 or 96 hours, and parasites were collected and conserved in Trizol. Every experiment was performed in triplicate. RNA was extracted from each sample and cDNA was obtained by reverse transcription with MMLV. RT-qPCR was performed with Sybr Green reagent and the primers indicated in each graph, using tubulin and actin as housekeeping controls. Data were normalized to each of the housekeeping controls and relative quantities to tachyzoite in each sample is plotted for each of the genes studied. GraphPad Prism was used to statisticaly analyze data, by two-way Anova. ***: $p < 0.0001$; **: $p < 0.01$; *: $p < 0.05$; ns: not significant.

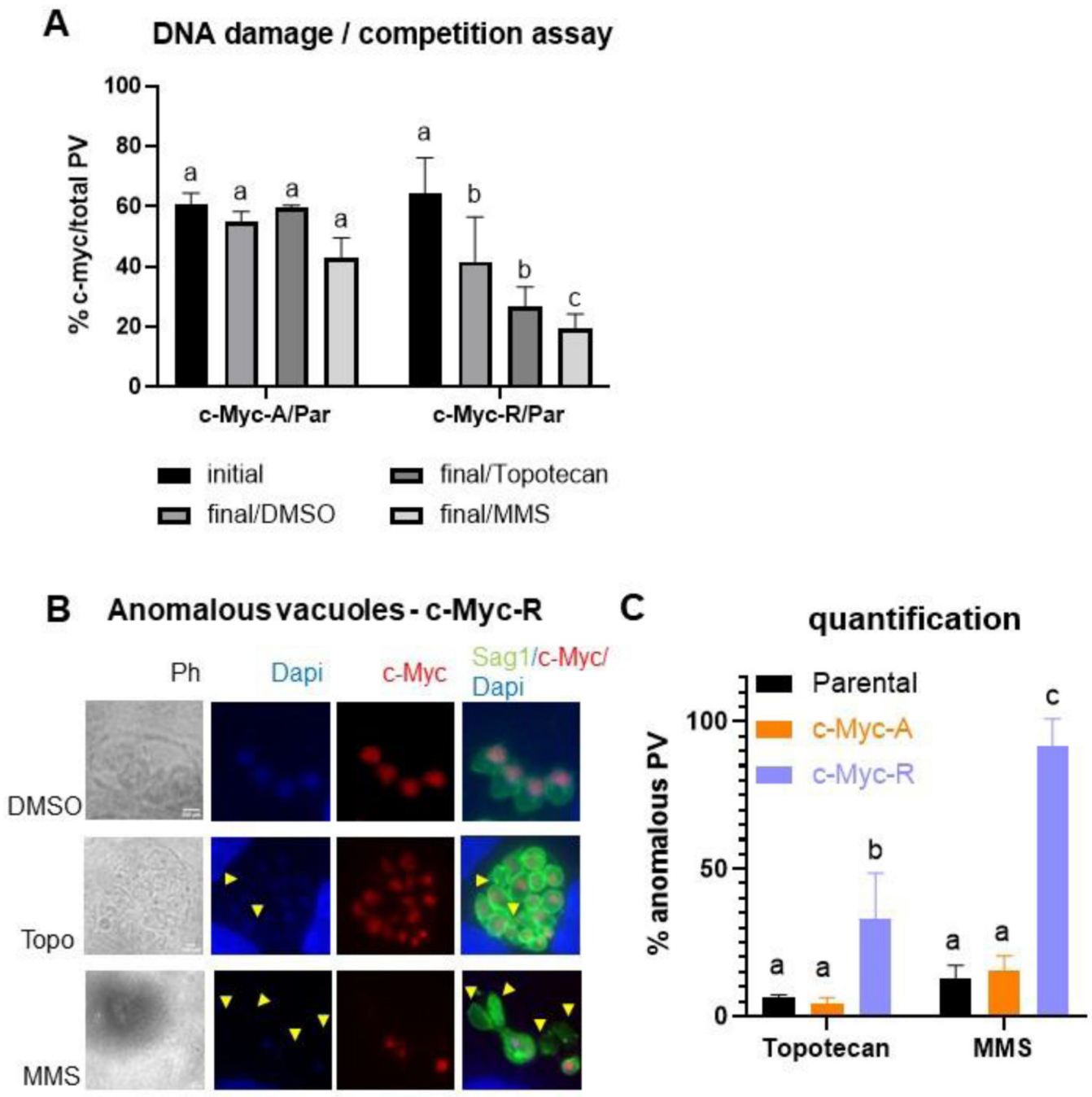

Figure 4. H2B.Z acetylation status is important for DNA damage sensitivity.

A. Competition assay after DNA damage induced by topotecan (20 μM) or MMS (50 μM). Competition assay and IFAs were performed using α–Sag1 to determine total vacuoles and α–c-Myc to determine the designated parasite clone, performed in three independent experiments in triplicate. Graph shown corresponds to one representative assay. Initial: % of c-Myc vacuoles of the total after 24 hours of infection with the mixture. Final: % of c-Myc vacuoles of the total after 72 hours of treatment with each drug or DMSO as control. c-Myc-A/Par: mixture of c-Myc-A with parental (RHΔ*hxgprt*) tachyzoites; c-Myc-R/Par:

mixture of c-Myc-R with parental (RHΔ*hxgprt*) tachyzoites. GraphPad Prism 8 statistical ANOVA analysis, multiple comparison where DMSO final is compared to initial in each case and drug data is compared to DMSO: a: ns; b: $p<0.05$; c: $p<0.01$. **B.** Vacuoles affected by drugs. Representative images of most affected parasites (c-Myc-R) following indicated drug treatment. DMSO images are included as control. Yellow arrowheads point to parasites with loss of genetic material. **C.** Quantification of anomalous vacuoles. Anomalous and normal vacuoles were counted in at least 50 randomly chosen fields. Results were plotted in GraphPad Prism 8 and statistical analysis by Multiple comparision was performed. a: ns; b: $p<0.05$; c: $p<0.001$.

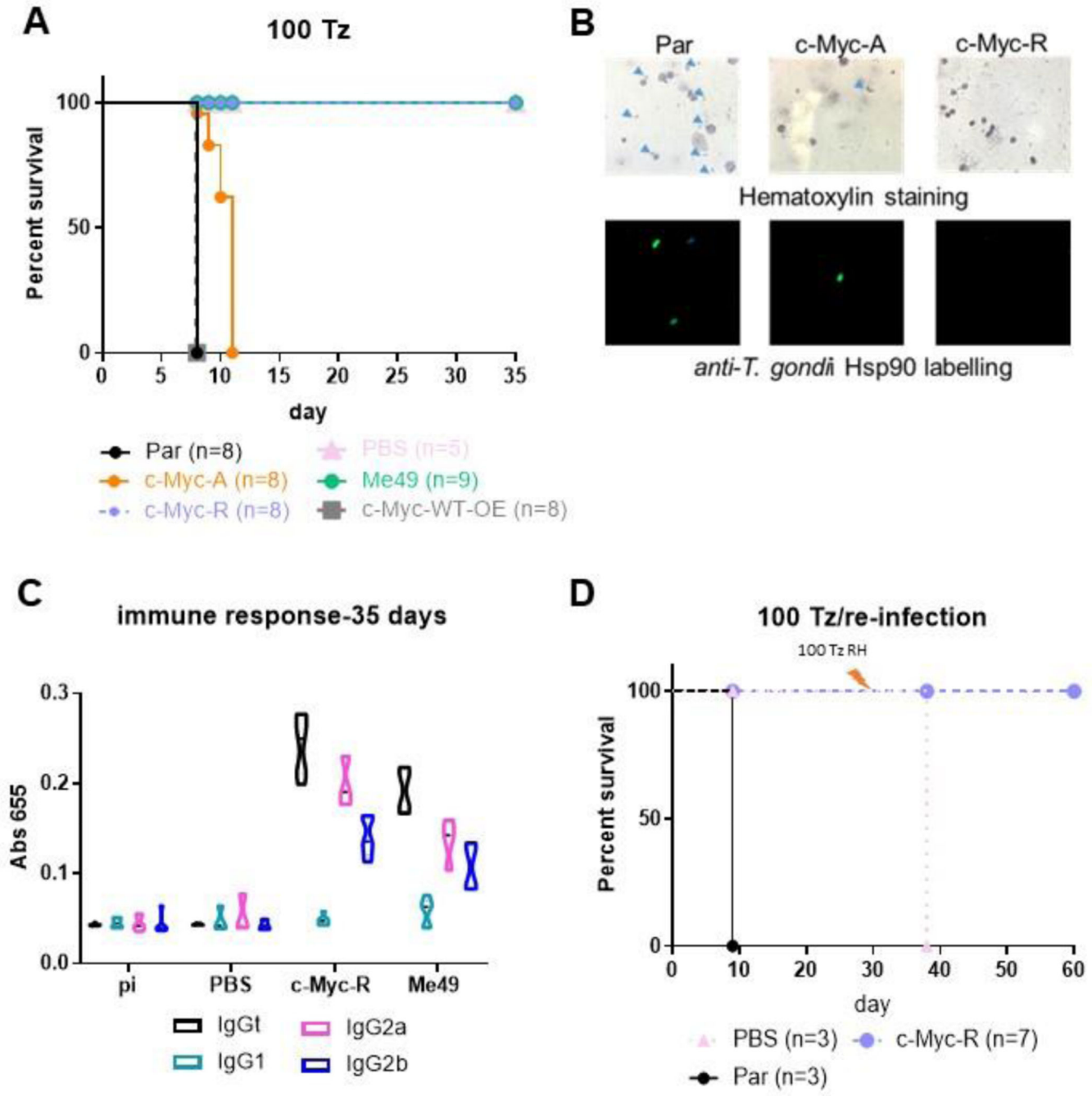

Figure 5. c-Myc-R tachyzoites are not virulent *in vivo* and elicit a protective immune response.

A. Survival assay. 10 mice C57BL/6 were intra-peritoneal infected with either 100 tachyzoites of parental (RHΔ*hxgprt*), and one clone of each KO line: c-Myc-R and c-Myc-A. As controls we also infected mice with c-Myc-WT-OE, vehicle (PBS), or Me49 tachyzoites (type II). The survival curve shown corresponds to one assay, representative of three independent experiments. **B.** Acute infection. At day 5, 2 mice of each group were sacrificed, and intra-peritoneal liquid was extracted and analyzed in the microscope, either by hematoxylin staining (upper panel), or by IFA with α-HSP90 antibody (lower panel).

Arrowheads in the upper panel show tachyzoites. **C.** Evaluation of immune response by ELISA. Blood samples were extracted from surviving mice at days 0 (Pi), 14, 21 and 35. Pooled sera from mice inoculated with PBS (negative control) or infected with Me49 (positive control) were assayed. Total IgG and subtypes (IgG2a, IgG2b and IgG1) were analyzed. Results at day 35 are shown on graph. **D.** Re-infection assay. The indicated number of mice were infected with 1,000 parental (Par) or c-Myc-R tachyzoites or inoculated with PBS. After 30 days, surviving mice were re-infected with 100 parental RH tachyzoites (indicated by the orange lightning bolt: “100 Tz”). The survival curve shown corresponds to one assay, representative of three independent experiments.

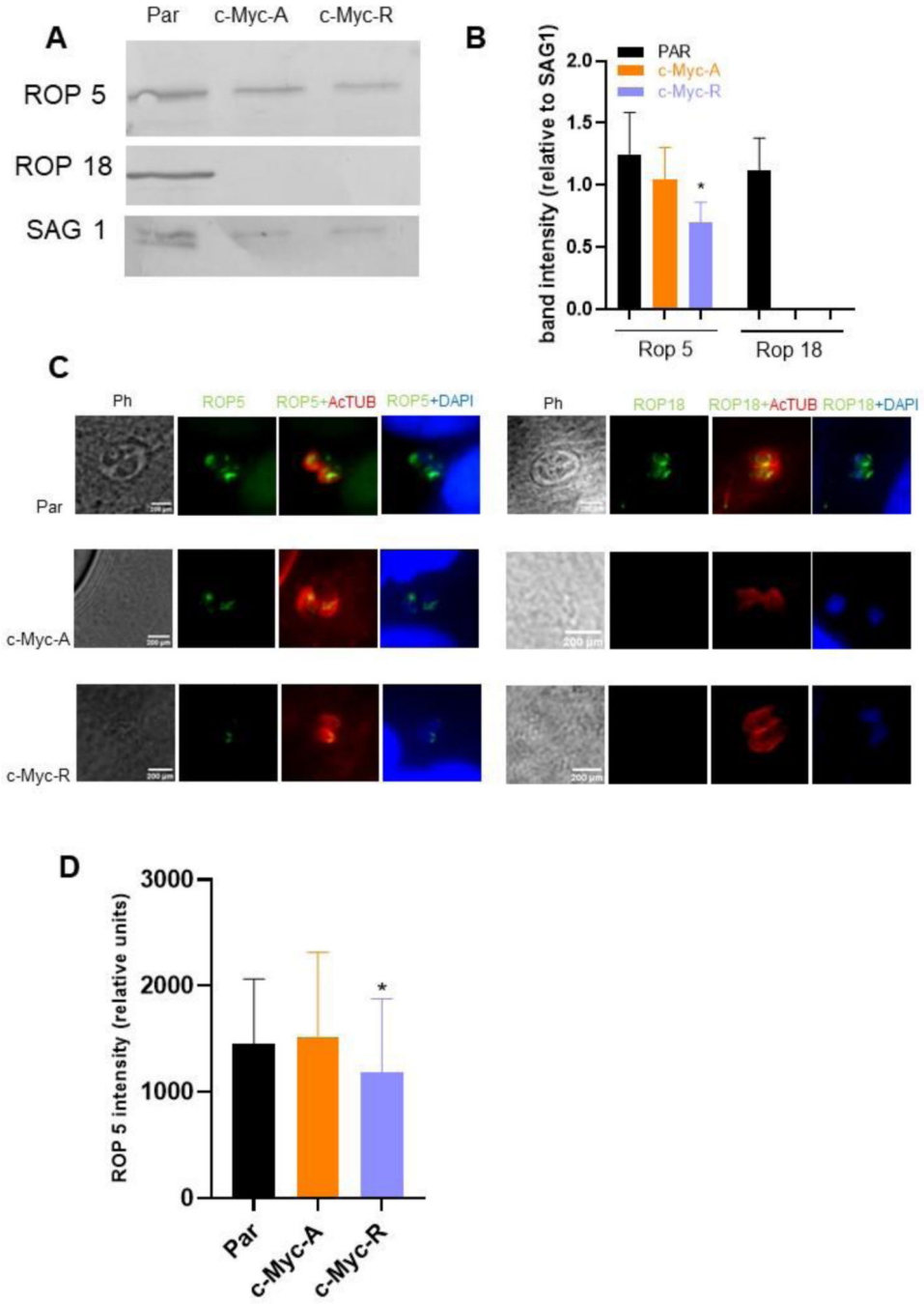

Figure 6. Expression of ROP proteins is affected by H2B.Z acetylation.

A. Western blot of Rop5 and Rop18, representative of three independent experiments, in which tachyzoite lysates of parental: Par (RHΔ*hxgprt*), c-Myc-A or c-Myc-R were probed with α–Sag1 (charge control), α–Rop5 and α–Rop18 antibodies. **B.** Quantification of band intensities relative to Sag1 in each lane. Image J software was employed to quantify relative intensities and graphed with GraphPad Prism 8. Average plus SD of three independent assays is represented. *: $p<0.05$. PAR: parental. **C.** Immunofluorescence assay. Slides of confluent Htert cells were infected with tachyzoites of parental: Par (RHΔ*hxgprt*), c-Myc-A

and c-Myc-R and fixed after 24 h for IFA analysis using α–Rop5 and α–Rop18 antibodies (green). AcTubulin (red) was used to stain parasites and DAPI for the nuclei. **D.** Rop5 intensity quantification. Image J software was used to quantify the antibody intensities in three independent experiments done in triplicate, examining at least 10 vacuoles per slide. The graph shows the average intensity in relative units; statistical analysis was performed by GraphPad Prism 8 software. *: $p<0.05$. Par: parental.

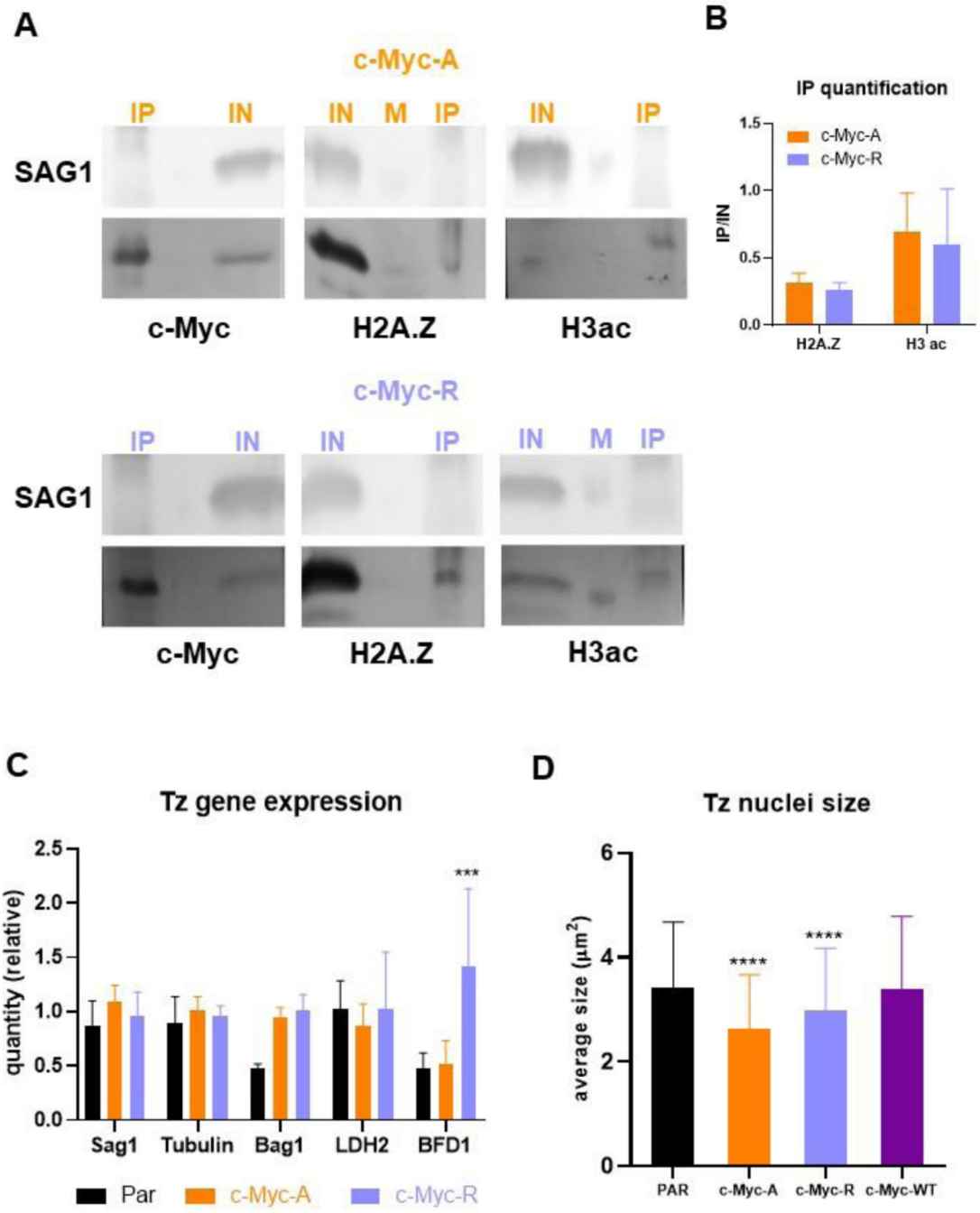

Figure 7. Nucleosome composition and chromatin structure is maintained in c-Myc-A and c-Myc-R.

A. Co-immunoprecipitation-WB analysis. Assays were performed in triplicate as explained in Materials and Methods. A representative western-blot is shown for c-Myc-A and c-Myc-R. IP: immunoprecipitation; IN: input. c-Myc: western blot probed with commercial α c-Myc antibody. H2A.Z: western blot probed with α–H2A.Z antibody performed in the lab.H3ac: western blot probed with commercial α–H3ac antibody. Sag1: western blot probed with α–Sag1 antibody. Color key: Orange for c-Myc-A; lilac for c-Myc-R. **B.** Quantification

of western blot band intensities. Image J software was used to quantify intensities of H3ac and H2A.Z IP bands relative to respective IN band intensities. Graph shows the relative intensities of three independent experiments as the average plus SD for each antibody and clone, with the same key color as before. GraphPad Prism 8 statistical analysis showed no significant differences between clones for both H3ac and H2A.Z quantification. **C.** Tachyzoites gene expression. Tachyzoites (Tz) of parental: Par (RHΔ*hxgprt*); c-Myc-A or c-Myc-R were freshly collected in triplicate and conserved in TriZol until processing. RNA was extracted from each sample and cDNA was obtained by reverse transcription with MMLV. RT-qPCR was performed using Sybr Green reagent with primers indicated in the graph and actin as housekeeping control. Data were normalized to actin and relative quantities to RH tachyzoites in each sample are plotted for each of the genes studied. GraphPad Prism was used to analyze data by two-way Anova. ***: $p < 0.0001$; ns: not significant. **D.** Tachyzoite nuclei size. Tachyzoites of parental: Par (RHΔ*hxgprt*), c-Myc-A, c-Myc-R or c-Myc-WT-OE were allowed to invade slides of hTert cells and replicate for 20 h; IFA was then performed with α-H2B.Z antibody to detect the nuclei. Image J software was used to measure the average nuclei size of at least 100 tachyzoites per slide in three independent experiments. Data were plotted and analyzed with GraphPad Prism 8 by two-way ANOVA. ****: $p < 0.0001$.

Table 1.

Identification of H2B.Z interacting proteins by pull-down assay with acetylated or non-acetylated N-terminal peptide.

Protein name	geneID	p Score	Peptides	Coverage (%)	Length (AAs)	N° pull-down	localization
Acetylated							
	TGME49_2626						nuclear
RRM	20	6.66	3	12	293	2	
Non-acetylated							
	TGME49_2182						nuclear
H3.3	60	9.98	5	21	136	2	
	TGME49_2198						nuclear
CDK	32	2.49	2	1	1260	2	
both							
	TGME49_2392						nuclear
H4	60	17.33	3	28	103	4	
	TGME49_2545						nuclear
GCN5-A	55	4.71	2	1	1186	4	
	TGME49_2242						nuclear
PHD	60	3.09	2	1	5657	2	
	TGME49_2909						cytosol
Clathrin hc	50	4.49	2	1	1731	2	
	TGME49_2090						cytoskeleton
Actin ACT1	30	19.8	3	10	376	2	
	TGME49_2216						cytoskeleton
β–tubulin	20	4.39	2	5	449	2	
	TGME49_2948						cytosol
eF1α	00	11.65	4	8	448	4	
	TGME49_2213						organelles
ACC1	20	53.36	16	8	2612	4	

Most representative peptides retrieved in two independent assays are listed.

Peptides: total number of peptides identified

Coverage displays the percentage of the protein sequences covered by identified peptides.

N° pull-down: number of assays in which peptide was retrieved

RRM: RNA recognition motif-containing protein; CDK: cyclin-dependent kinase regulatory subunit protein; GCN5-A: histone lysine acetyltransferase GCN5-A; PHD: PHD-finger domain-containing protein; Clathrin hc: Clathrin heavy chain; eF1α: elongation factor 1-alpha; ACC1: acetyl-CoA carboxylase

The raw data of all mass spectra had been submitted to the MassIVE (https://massive.ucsd.edu/; Project accession: MassIVE MSV000091226).